INVESTIGATION OF CERTAIN ASPECTS OF THE CAPACITOR COMMUTATED CONVERTER

by
Amir H. Hashim

A thesis submitted to
Faculty of Graduate Studies
in Partial Fulfilment of the Requirements for
Degree of Master of Science

Department of Electrical Engineering
UNIVERSITY OF MANITOBA
Winnipeg, Manitoba, Canada
October 1996

ISBN 0-612-16154-4

Name AMIR HISHAM HASHIM

Dissertation Abstracts International and *Masters Abstracts International* are arranged by broad, general subject categories. Please select the one subject which most nearly describes the content of your dissertation or thesis. Enter the corresponding four-digit code in the spaces provided.

SUBJECT TERM

ELECTRONICS AND ELECTRICAL

SUBJECT CODE 0544

UMI

Subject Categories

THE HUMANITIES AND SOCIAL SCIENCES

COMMUNICATIONS AND THE ARTS
Architecture 0729
Art History 0377
Cinema 0900
Dance 0378
Design and Decorative Arts 0389
Fine Arts 0357
Information Science 0723
Journalism 0391
Landscape Architecture 0390
Library Science 0399
Mass Communications 0708
Music 0413
Speech Communication 0459
Theater 0465

EDUCATION
General 0515
Administration 0514
Adult and Continuing 0516
Agricultural 0517
Art 0273
Bilingual and Multicultural 0282
Business 0688
Community College 0275
Curriculum and Instruction 0727
Early Childhood 0518
Elementary 0524
Educational Psychology 0525
Finance 0277
Guidance and Counseling 0519
Health 0680
Higher 0745
History of 0520
Home Economics 0278
Industrial 0521
Language and Literature 0279
Mathematics 0280
Music 0522
Philosophy of 0998
Physical 0523
Reading 0535
Religious 0527
Sciences 0714
Secondary 0533
Social Sciences 0534
Sociology of 0340
Special 0529
Teacher Training 0530
Technology 0710
Tests and Measurements 0288
Vocational 0747

LANGUAGE, LITERATURE AND LINGUISTICS
Language
- General 0679
- Ancient 0289
- Linguistics 0290
- Modern 0291
- Rhetoric and Composition 0681

Literature
- General 0401
- Classical 0294
- Comparative 0295
- Medieval 0297
- Modern 0298
- African 0316
- American 0591
- Asian 0305
- Canadian (English) 0352
- Canadian (French) 0355
- Caribbean 0360
- English 0593
- Germanic 0311
- Latin American 0312
- Middle Eastern 0315
- Romance 0313
- Slavic and East European 0314

PHILOSOPHY, RELIGION AND THEOLOGY
Philosophy 0422
Religion
- General 0318
- Biblical Studies 0321
- Clergy 0319
- History of 0320
- Philosophy of 0322

Theology 0469

SOCIAL SCIENCES
American Studies 0323
Anthropology
- Archaeology 0324
- Cultural 0326
- Physical 0327

Business Administration
- General 0310
- Accounting 0272
- Banking 0770
- Management 0454
- Marketing 0338

Canadian Studies 0385
Economics
- General 0501
- Agricultural 0503
- Commerce-Business 0505
- Finance 0508
- History 0509
- Labor 0510
- Theory 0511

Folklore 0358
Geography 0366
Gerontology 0351
History
- General 0578
- Ancient 0579
- Medieval 0581
- Modern 0582
- Church 0330
- Black 0328
- African 0331
- Asia, Australia and Oceania 0332
- Canadian 0334
- European 0335
- Latin American 0336
- Middle Eastern 0333
- United States 0337

History of Science 0585
Law 0398
Political Science
- General 0615
- International Law and Relations 0616
- Public Administration 0617

Recreation 0814
Social Work 0452
Sociology
- General 0626
- Criminology and Penology 0627
- Demography 0938
- Ethnic and Racial Studies 0631
- Individual and Family Studies 0628
- Industrial and Labor Relations 0629
- Public and Social Welfare 0630
- Social Structure and Development 0700
- Theory and Methods 0344

Transportation 0709
Urban and Regional Planning 0999
Women's Studies 0453

THE SCIENCES AND ENGINEERING

BIOLOGICAL SCIENCES
Agriculture
- General 0473
- Agronomy 0285
- Animal Culture and Nutrition 0475
- Animal Pathology 0476
- Fisheries and Aquaculture 0792
- Food Science and Technology 0359
- Forestry and Wildlife 0478
- Plant Culture 0479
- Plant Pathology 0480
- Range Management 0777
- Soil Science 0481
- Wood Technology 0746

Biology
- General 0306
- Anatomy 0287
- Animal Physiology 0433
- Biostatistics 0308
- Botany 0309
- Cell 0379
- Ecology 0329
- Entomology 0353
- Genetics 0369
- Limnology 0793
- Microbiology 0410
- Molecular 0307
- Neuroscience 0317
- Oceanography 0416
- Plant Physiology 0817
- Veterinary Science 0778
- Zoology 0472

Biophysics
- General 0786
- Medical 0760

EARTH SCIENCES
Biogeochemistry 0425
Geochemistry 0996
Geodesy 0370
Geology 0372
Geophysics 0373
Hydrology 0388
Mineralogy 0411
Paleobotany 0345
Paleoecology 0426
Paleontology 0418
Paleozoology 0985
Palynology 0427
Physical Geography 0368
Physical Oceanography 0415

HEALTH AND ENVIRONMENTAL SCIENCES
Environmental Sciences 0768
Health Sciences
- General 0566
- Audiology 0300
- Dentistry 0567
- Education 0350
- Administration, Health Care 0769
- Human Development 0758
- Immunology 0982
- Medicine and Surgery 0564
- Mental Health 0347
- Nursing 0569
- Nutrition 0570
- Obstetrics and Gynecology 0380
- Occupational Health and Safety 0354
- Oncology 0992
- Ophthalmology 0381
- Pathology 0571
- Pharmacology 0419
- Pharmacy 0572
- Public Health 0573
- Radiology 0574
- Recreation 0575
- Rehabilitaion and Therapy 0382
- Speech Pathology 0460
- Toxicology 0383

Home Economics 0386

PHYSICAL SCIENCES
Pure Sciences
Chemistry
- General 0485
- Agricultural 0749
- Analytical 0486
- Biochemistry 0487
- Inorganic 0488
- Nuclear 0738
- Organic 0490
- Pharmaceutical 0491
- Physical 0494
- Polymer 0495
- Radiation 0754

Mathematics 0405
Physics
- General 0605
- Acoustics 0986
- Astronomy and Astrophysics 0606
- Atmospheric Science 0608
- Atomic 0748
- Condensed Matter 0611
- Electricity and Magnetism 0607
- Elementary Particles and High Energy 0798
- Fluid and Plasma 0759
- Molecular 0609
- Nuclear 0610
- Optics 0752
- Radiation 0756

Statistics 0463

Applied Sciences
Applied Mechanics 0346
Computer Science 0984
Engineering
- General 0537
- Aerospace 0538
- Agricultural 0539
- Automotive 0540
- Biomedical 0541
- Chemical 0542
- Civil 0543
- Electronics and Electrical 0544
- Environmental 0775
- Industrial 0546
- Marine and Ocean 0547
- Materials Science 0794
- Mechanical 0548
- Metallurgy 0743
- Mining 0551
- Nuclear 0552
- Packaging 0549
- Petroleum 0765
- Sanitary and Municipal 0554
- System Science 0790

Geotechnology 0428
Operations Research 0796
Plastics Technology 0795
Textile Technology 0994

PSYCHOLOGY
General 0621
Behavioral 0384
Clinical 0622
Cognitive 0633
Developmental 0620
Experimental 0623
Industrial 0624
Personality 0625
Physiological 0989
Psychobiology 0349
Psychometrics 0632
Social 0451

THE UNIVERSITY OF MANITOBA

FACULTY OF GRADUATE STUDIES

COPYRIGHT PERMISSION

INVESTIGATION OF CERTAIN ASPECTS OF THE CAPACITOR COMMUTATED CONVERTER

BY

AMIR H. HASHIM

A Thesis/Practicum submitted to the Faculty of Graduate Studies of the University of Manitoba in partial fulfillment of the requirements for the degree of

MASTER OF SCIENCE

ACKNOWLEDGEMENTS

Innumerable thanks to Dr. A Gole for all his help towards the completion of this thesis. The friendly staff of the Power Tower U of M, HVDC Research Centre and Teshmont Consultants, Winnipeg, Canada. My friends who have always been there and and those who would have but could not possibly make it. Finally, my family who have always been there on the other end of the phone. Without any of you, this thesis would not have been completed. Thank you.

ABSTRACT

The availability of more feasible power generation far from load centres, amongst other things, have prompted the use of HVDC links. With increasing system complexity, HVDC links must be designed to be more reliable and robust. This has prompted the emergence of the Capacitor Commuted Converter (CCC).

Unlike the conventional converter which relies on the ac line voltage, the CCC commutation voltage is derived from the sum of the line voltage and the net capacitor voltages. This enhances the commutation angle and provides a certain degree of immunity from ac side disturbances. The CCC may also be operated at a higher firing angle and reactive power consumption can be minimised.

This thesis has examined the CCC concept so as to determine its operational capabilities. Some new components have been also introduced, namely, the Capacitor DC Modulation and Active Filters. Results indicate that the CCC valve current ratings can be minimised with HVDC systems with long cables, capacitors with small X_c will give good results whilst minimising costs, and system stability is improved amongst other things.

Table of Contents

List of Figures

List of Tables

Nomenclature

α = firing order

μ = overlap angle

γ = extinction angle

CCC = Capacitor Commutated Converter

CC = Converter Capacitors

V_{capA} = Voltage of CC in Phase A

V_{capB} = Voltage of CC in Phase B

V_{capC} = Voltage of CC in Phase C

THD = Total Harmonic Distortion

GTO = Gate Turn Off Devices

CEA = Constant Extinction Angle Control

CVC = Constant Voltage Control

CCurrC = Constant Current Control (usually called CC but will conflict with Converter Capacitors in this thesis)

CHAPTER ONE

INTRODUCTION

Conventional HVDC converters rely on line voltages for the commutation process. With regards to that, valves are fired with an angle margin to ensure successful turn off or turn on and hence avoid commutation failure . This leads to a lagging line current which would mean reactive power consumption. If valves can be fired with a smaller margin (i.e.very near the voltage zero crossing), reactive power consumption can be minimised. Of course, if we look at inverter operation, if we can fire the valve after voltage zero crossing, the inverter can actually supply reactive power.

Further, HVDC schemes employing power transfer via long submarine cables are becoming more important due to the availability of more feasible power generation in regions across large bodies of water with respect to the load centres. A case in point is the Bakun hydro electric plan in East Malaysia with the a total generating capacity of 2400 MW. This involves a planned 650 km of submarine cables.

In case of a fault on the a.c. side, the discharge current from the long cable capacitance is uncontrollable. The rectifier is effectively decoupled from the inverter due to the very large capacitance inherent in the long cable. Certain control strategies for long cable d.c. schemes [1] have been forwarded such as the variable gamma control but this would mean firing with a large nominal gamma (to be able to shift to a smaller gamma during contingencies and hence increase inverter voltage), hence increasing reactive power demand. Indeed, an increase in reactive power consumption means the need for a larger reactive power source such as capacitor banks on filters. This would lead to a higher load rejection overvoltage, which will impact the cost.

Fig 1.1 shows the 6 - pulse Graetz bridge for conventional HVDC conversion. Thyristor firing is in the usual fashion of T1, T2,..,T6, T1.. The datum for the firing angle alpha is the phase crossover. The angle μ is the measure of the commutation interval where both valves (the on going valve and the off going valve, say T1 commutating to T3) conduct as they move towards an equilibrium state. γ is the 'rest time' of the valve before it is forward biased again. The definition for γ is the angle between the forward current zero crossing and the positive going voltage zero crossing of the particular phase. In this case, $\alpha + \mu + \gamma$ can only be a maximum of 180 degrees.

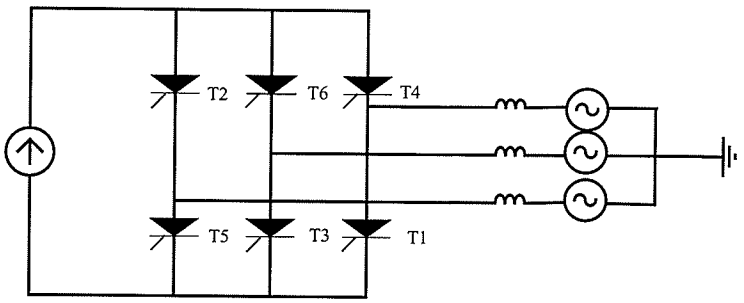

Fig 1.1 Equivalent Circuit of a Conventional Inverter

The Self Commutated Converter (SCC) or a Capacitor Commutated Converter (CCC) is an artificial means of increasing the ability to fire at higher angles while maintaining proper converter operation. The concept of forced/artificial commutation has been introduced earlier [2] but has never been employed in a high power transmission application. Another possibility is to use gate turn-off device based voltage source converter. However, their investigation is outside the scope of this thesis.

1.1 Capacitor Commutated Converter

A CCC employs a series capacitor (Fig 1.2) between the converter and the converter transformer. For practical purposes, we shall call the capacitors, Converter Capacitors (CC) throughout this thesis. The inverter does not rely on the a.c. system wholly for commutation as the capacitors will provide the added commutation voltage for the valves as it is charged up by the converter current.

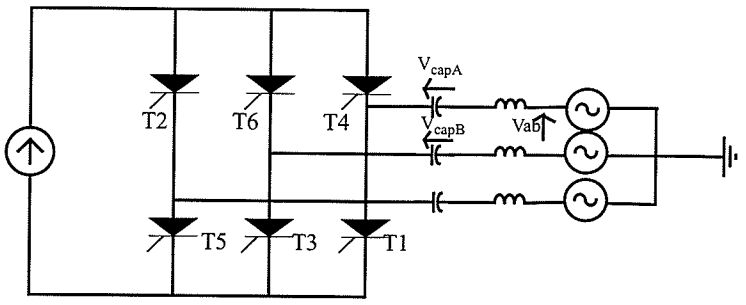

Fig 1.2 Equivalent Circuit of a CCC

1.2 CCC Operation

Fig. 1.3 shows certain waveforms of the CCC in an attempt to acquaint the reader to the operation. The only difference of the CCC from the previous circuit is the appearance of the CC (Converter Capacitor) between the valve group and the converter transformer in each phase. The d.c. current is assumed constant and will charge the CC proportionally. The capacitor voltage is dictated by the d.c. current integral and of course, the value of the capacitors.

$$V_{cap} = \frac{1}{C}\int Idt$$

which gives a peak capacitor voltage of

$$V_{peakcap} = \frac{Id}{3fC}$$

With respect to Figure 1.3, T3 is about to take over conduction from T1 (overlap is neglected in this analysis). At point A, assume that T1 and T2 are conducting. Now let us fire T3 to take over from T1, the capacitors in the respective phases are in the correct

polarity for commutation. The transfer voltage for this process would be:

$$\text{Commutation Voltage} = V_{ab} + V_{capA} - V_{capB}$$

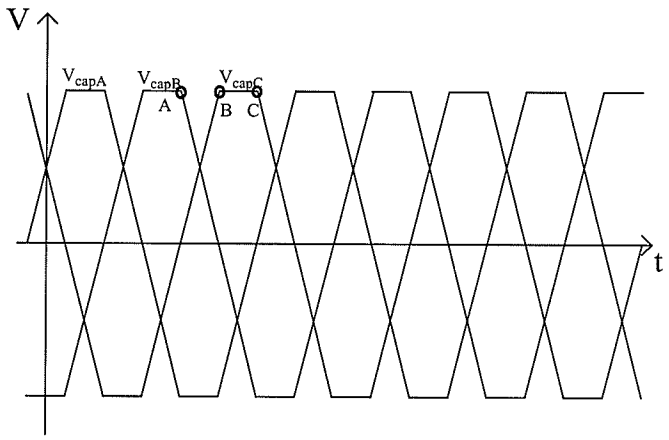

Fig 1.3 Capacitor Voltages

As the commutation of T1 takes place, the voltage of CC_b decreases towards zero as the phase B starts to conduct and the capacitor is discharging. Voltage of CC_a stays constant as current has stopped flowing through it after the overlap period (not seen in this diagram). Voltage of CC_c rises as constant current flows through it during the conduction of T2 and will stop rising when T4 takes over T2. By then, V_{capC} will be charged fully in the positive direction and as no valve is conducting in phase C, the voltage on CC_c was constant (point B). This voltage is then ready to commutate T3 for T5 at point C.

The CCC scheme also reduces the need for providing reactive power to an HVDC converter [2]. Traditionally, reactive power compensation, in general, was achieved by

means of shunt a.c. filters. Since the reactive power varies, the a.c. filters are divided into several banks and each bank is connected to the a.c. system accordingly based on the required reactive power. This arrangement translates into the need for extra breakers and monitoring equipment, leading to an increase in costs. Further, the CCC concept can separate the function of harmonic filtering and reactive power compensation by the a.c. filters, thereby reducing the rating the a.c. filters. It has been reported by Asplund et al [3], that the CCC would work well with the implementation of active filtering or continuously tuned a.c. filters. This concept would be examined in this report.

The CCC capacitor is in series with the converter and thus can provide a reactive power compensation proportional to the load current of the converter. This eliminates the need for the extra equipment and may prove advantageous in highly built up areas.

1.3 Benefits of CCC

a) CCC will improve commutation failure performance as the capacitor will introduce a commutation voltage from the charging of the line currents from the a.c. system and the converter[4]. If the series capacitor has enough voltage to commutate the valves, the firing angle can be advanced beyond 180 degrees and theoretically even supply reactive power.

b) The commutation voltage from the series capacitor will result in positive inverter impedance[4]. The increase in direct current will result in an inverter d.c. voltage increase. This will be advantageous for an inverter operating at minimum commutation

margin control and will enhance stability. Further, the positive inverter impedance will aid recovery in a system with a long dc submarine cable if the cable discharges during a.c. faults.

c) As mentioned earlier, load rejection overvoltages will be minimised. as the a.c. filter rating can be reduced. Smaller shunt filters will also reduce risk of low order harmonics.

d) The converter will be more stable for the same power rating due to cancellation of the reduction of the transformer reactance by the series capacitor. In this case, the cancellation of the transformer inductance will not have an adverse effect on the short circuit current limiting capabilities as the CC are also a limiting component by introducing a counter voltage.

e) The rating of the converter transformer can be reduced by reducing the line-line voltage on the converter side as the reactive power flow through it is minimised.

f) Inversion into a weak system is easier.

1.4 The Series Capacitor

a) The capacitor is d.c. current charged and this quantity remains relatively constant in the system, giving a reliable dynamic operation.

b) The capacitor is located between the transformer and the valve winding to allow full control of capacitor currents and also to eliminate ferroresonance problems [3].

c) Steady state operating voltage of the capacitor is determined by direct current. If the direct current increases, the operating voltage of the capacitor will also increase. The capacitor must be protected by arrestors against overvoltages.

d) The capacitors will reduce valve short circuit currents due to voltage drop across the capacitor as the CC will set up a counter voltage [4] as it is being charged up by the short circuit current. However, the voltage stresses on the valve will be higher compared to conventional converters.

e) Overlap angle will be reduced with respect to conventional converters as the commutation capacitor voltage will add to the a.c. line voltage. A reduced overlap angle will increase the harmonic content by about 20%[4].

f) A new notation for gamma and alpha must be introduced. Traditionally, $\alpha + \gamma + \mu$ = 180 degrees. However, with the CCC, the CC (converter capacitor) will provide additional commutation voltage and allow for firing of well beyond 180 degrees. This may mean a negative gamma. Also, we have to specify the commutation margin 'real' gamma to indicate the rest time of the valve before it sustains another forward bias. Fig. 1.4 (on the next page) shows that apparent gamma is negative if we fire after 180 degrees.

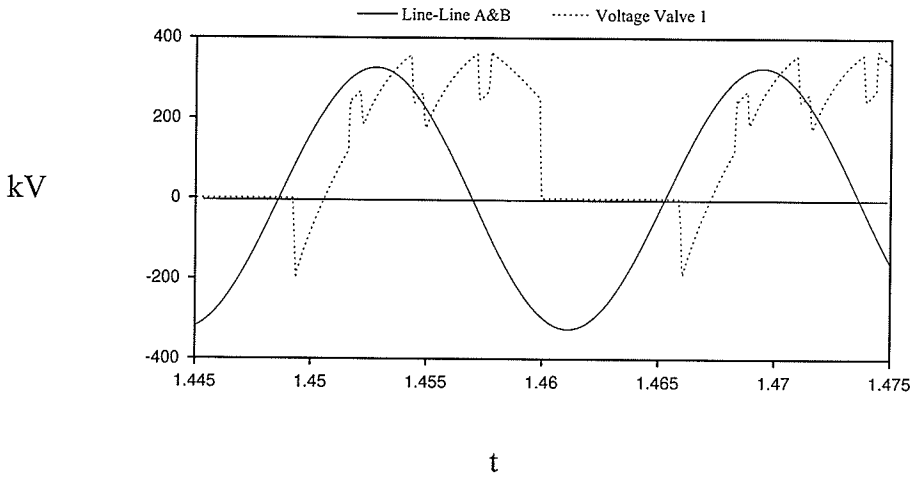

Fig 1.4 Negative Apparent Gamma at High Firing Angles

1.5 Requirements of a CCC Scheme

As argued by Gole and Menzies [5] the CCC must satisfy most, if not all, of the requirements below.

a) High reliability and improvement in commutation failure performance in cases of a.c. side fault.

b) Minimal stress to converter components due to reduced valve short circuit current. However, it should be noted that this is not straightforward as a study by Jonsson [4] has shown that voltage stresses will be higher for the CCC. This is because the CCC will have higher extinction voltage steps and combined with the shorter commutation interval will

lead to higher commutation overvoltages, leading to higher requirements of snubber circuits and valve arrestors.

c) Fast change of alpha must be possible. The CC should not slow down the rate of change for alpha to accommodate for transient response.

This thesis will attempt to model the CCC as accurately as possible by including new components such as active filters and capacitor modulation controls, to determine its strength and weaknesses and thus produce a solid assessment of the scheme. Chapter 2 will analyse the basic circuit operation. Chapter 3 will introduce the components which were used in simulating the CCC. Results of the tests done on the CCC will be found in Chapter 4. Chapter 5 will be the conclusion. It is hoped that the reader will appreciate the CCC more with the findings accumulated within these pages.

CHAPTER TWO

BASIC CIRCUIT ANALYSIS

This chapter will examine the basic properties of the CCC using a simplified circuit as shown in Fig 1.2. A 6 pulse bridge converter is connected to an infinite bus without any shunt filtering/reactive power compensation to illustrate the main differences between the CCC and the conventional converter. A constant direct current is applied to simulate the continuous dc current. Thus, dc current harmonic effects are ignored in this first approximation.

2.1 DC Voltage Range

A simulation of a 6 pulse bridge with a constant current source was done with varying alpha orders. It is expected that the CCC can be operated in all four quadrants (0 to 360 degrees) with no difficulty. Fig 2.1 below shows the variation of dc voltages and measured gamma as the CCC is slowly shifted through alpha orders 0 to 200 degrees. It is shown that at 90 degrees, the voltage is near enough to 0V. This discrepancy is due to the overlap angle existing in the bridge. The plant data for the plot below and the following

plots are included in Appendix A unless otherwise stated. Figure 2.1 below also suggests that the controls are not very sensitive at the 180 degrees region as shown by the limited change of dc voltage with respect to alpha orders.

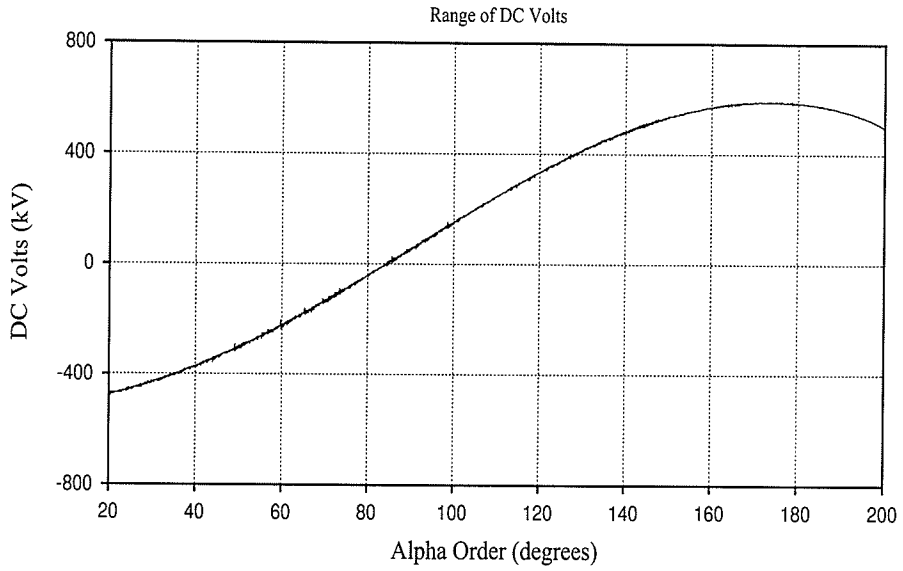

Fig 2.1 DC Voltage Range

2.2 Commutation Angle

The commutation angle plot below shows that γ can be reduced to a negative value with respect to line voltage at high firing angles. This is because the converter capacitor (CC) adds to the commutation voltage and also introduces a phase shift with respect to the line voltage. This simply means that the valves turn off *after* the line voltage crosses zero since the line voltage is no longer directly responsible for commutation. Fig

2.2 illustrates the apparent gamma range with increasing magnitude of the commutation capacitor X_c.

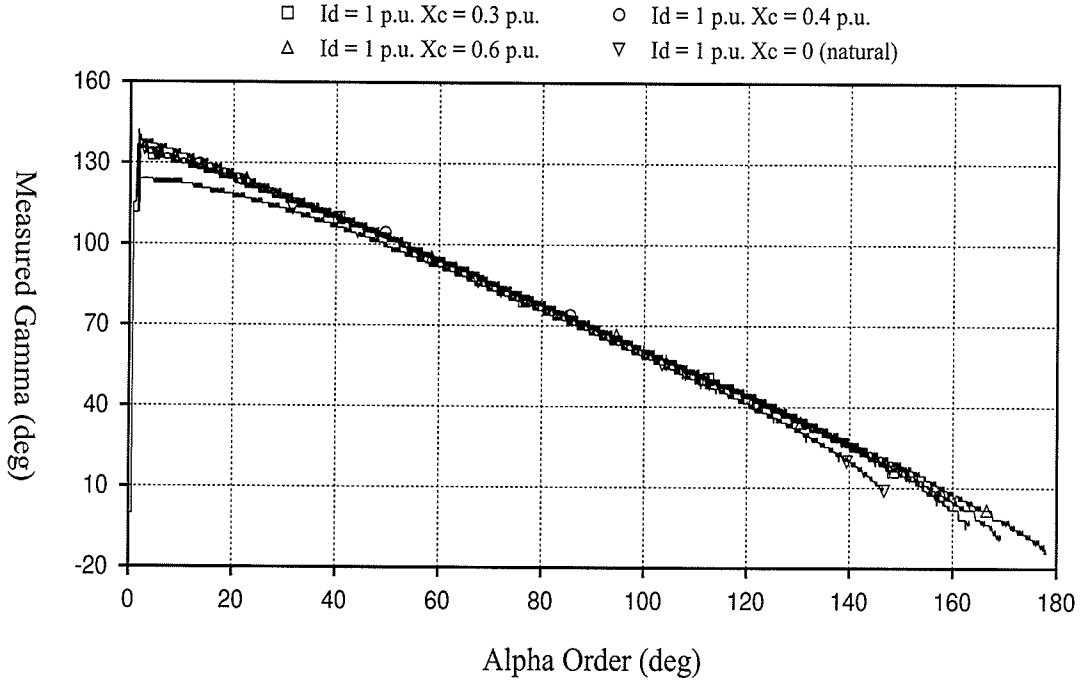

Fig 2.2 Commutation Angle Range (Apparent γ)with Respect to X_c

The plot above also clearly shows that operation of the CCC can be extended into the 180 degree firing angle region with increasing X_c values of capacitor, and hence produce reactive power if need be. Values of gamma within the normal operating range, increases about 10 degrees from the naturally commutated converter. This increase in gamma margin would provide extra robustness in commutation failure performance. The curve for the naturally commutated inverter should theoretically end at 180 degrees before

commutation failure, but in this case, the EMTDC model simulated a real inverter whereby commutation failure occurred at about gamma equals 9 degrees.

The author would also like to point out that the commutation angle measured above is the apparent gamma, whereby gamma is measured between valve zero negative crossing and the line voltage. That is the reason the inverter is still operational at 'negative' gamma. The real gamma however, is measured from the reverse biased period of the valve and this must always have a positive value to prevent commutation failure.

2.3 Real and Reactive Power

The plots for the real power and the reactive power is shown below in Fig 2.3 for a 1 p.u capacitor.

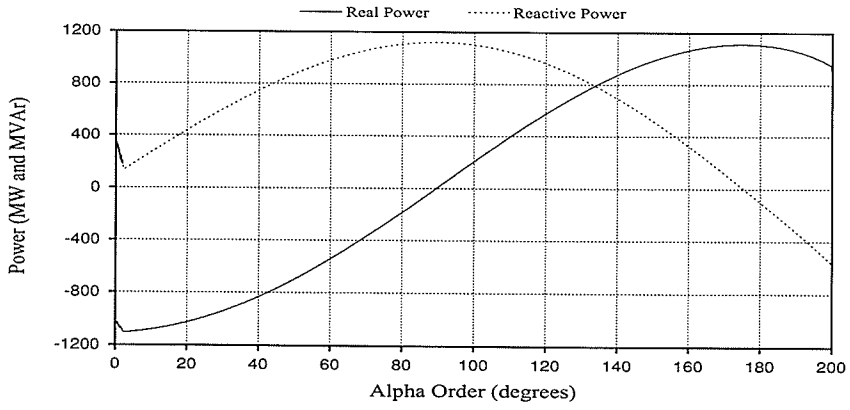

Fig 2.3 Real and Reactive Power

Real power transmission can be increased at high firing angles. Conventionally, we could not operate at these high firing angle regions due to the commutation angle limitations [6]. However, the real advantage of the CCC is really the reduction in reactive power demand at these operating region. Plot above shows that if we could operate at about 175 degrees, we would not need to compensate the CCC at all. Theoretically, Q = 0 should be at 180 degrees but due to the overlap angle, Q = 0 point occurs at a lower value of α.

2.4 DC Voltage Calculation

The mean direct voltage calculation has been derived by Reeve, Baron and Hanley [2]. The derivation can be made from taking into account a) the commutation period and b) when two valves are conducting. The resulting expression (inverter convention) is shown below,

$$V_d = -\left(\left(\frac{3V_{ll}}{\sqrt{2}\pi}\right)(\cos\alpha + \cos(\alpha+\mu)) + \left(\frac{\pi}{3} - \frac{3\mu}{4}\right)(\Delta V_2 - \Delta V_1)\right)$$

where

ΔV_1= change of the capacitor voltage in the outgoing phase during overlap.

$$= \frac{2\left(A\mu - B\sin\mu + \dfrac{D}{\cos(\mu-1) - \left(\dfrac{E\omega}{\omega_o}\right)\sin\left(\dfrac{\omega_o\mu}{\omega}\right)} + \dfrac{G\omega}{\omega_o}\left(\cos\left(\dfrac{\omega_o\mu}{\omega}\right)\right) - 1\right)}{\omega C\left(1 + \cos\left(\dfrac{\omega_o\mu}{\omega}\right)\right)}$$

where

$$A = \frac{Id}{2}$$

$$B = \frac{\sqrt{2}V_l \cos\alpha}{2L\left(\omega_o^2 - \omega^2\right)}$$

$$D = \frac{(-\sqrt{2})\,V_l \omega \sin\alpha}{2L\left(\omega_o^2 - \omega^2\right)}$$

$$E = \frac{(-\sqrt{2})\,V_l \omega \sin\alpha}{2L\left(\omega_o^2 - \omega^2\right)} - \frac{Id}{2}$$

$$G = \frac{\sqrt{2}V_l \cos\alpha}{2L\left(\omega_o^2 - \omega^2\right)} + \frac{Id\pi\omega_o}{3\omega}$$

ΔV_2 = change of the capacitor voltage in the incoming phase during overlap.

$$= \frac{Id\mu}{\omega C} - \Delta V_1$$

μ = overlap angle

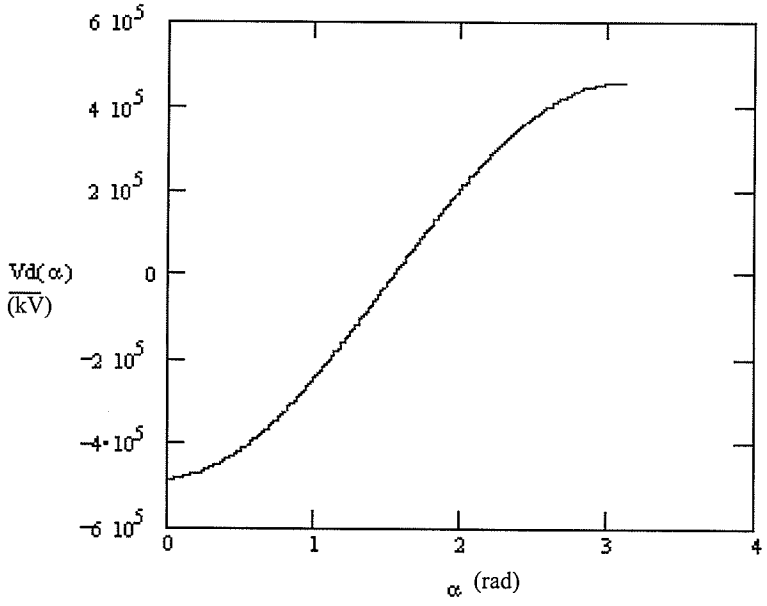

Fig 2.4 DC Voltage Range from the Above Equations

The curve above does not exactly match the PSCAD plot earlier as a constant overlap angle was used. Appendix B will show dc voltage calculation (in rectifier convention) as derived with assistance from A. M. Gole, with exact overlap angle.

2.5 Calculation of Overlap Angle

The overlap angle for a CCC is still defined as the time it takes for the off-going valve to completely commutate, (i.e. current reaches zero) as in a conventional converter. A mathematical model was developed to derive mju based on the simplified circuit in Fig 2.5 below. The equations and diagram in Appendix B show the steps of calculating the overlap angle in Mathcad.

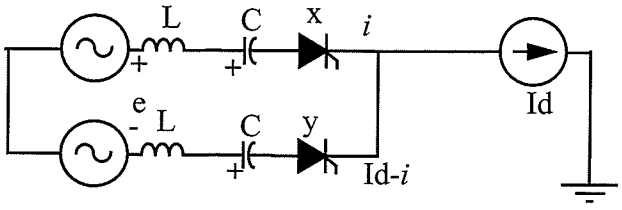

Fig 2.5 Simplified Circuit for Mju Calculation

Let

$$E = \sqrt{2} \cdot V \cdot \sin(\omega \cdot t + \alpha)$$

$$e = (E \cdot \sin(\omega \cdot t + \alpha))/2$$

$$e - \left(L \cdot \frac{di}{dt}\right) - Vx + Vy + L\frac{d}{dt}(Id - i) = 0$$

$$e - 2L\frac{di}{dt} - Vx + Vy = 0$$

(eq 2.1)

Also

$$i = C\frac{d}{dt}Vx$$

and

$$Id - i = C\frac{d}{dt}Vy$$

(eq 2.2)

If we differentiate eq. 2.1, we get

$$\frac{d}{dt}e - 2L\frac{d^2}{dt^2}i - \frac{d}{dt}Vx + \frac{d}{dt}Vy = 0$$

Substituting above equations into the derivative of 2.1, gives

$$E\omega\cos(\omega t + \alpha) - 2L\frac{d^2}{dt^2}i - \frac{i}{C} + \frac{Id - i}{C} = 0$$

$$E\omega\cos(\omega t + \alpha) + \frac{Id}{C} = 2L\frac{d^2}{dt^2}i + \frac{2}{C}$$

dividing by 2L gives

$$\frac{E\omega\cos(\omega t + \alpha)}{2L} + \frac{Id}{2LC} = \frac{d^2}{dt^2}i + \frac{i}{LC}$$

or

$$\frac{d^2}{dt^2}i + \frac{1}{LC}i = \frac{E\omega\cos(\omega t + \alpha)}{2L} + \frac{Id}{2LC}$$

(eq. 2.3)

2.5.1 Homogenous Solution

$$\frac{d^2}{dt^2}i + \frac{1}{LC}i = 0$$

$$i_{homo} = A\cos\left(\frac{1}{\sqrt{LC}}t\right) + B\sin\left(\frac{1}{\sqrt{LC}}t\right)$$

$$i_{homo} = A\cos(\omega_0 t) + B\sin(\omega_0 t)$$

where

$$\omega_o = \frac{1}{\sqrt{LC}}$$

2.5.2 Particular solution

a) For $\frac{Id}{2LC}$ excitation, we have a d.c. quantity and the second order derivative of current will be reduced to zero, hence,

$$0 + \frac{1}{LC}i_{pa} = \frac{Id}{LC}$$

$$i_{pa} = \frac{Id}{2}$$

b) For $\frac{E\omega\cos(\omega t + \alpha)}{2L}$ excitation, we use phasors and hence

$$i_{pb} = \frac{E\omega\cos(\omega t + \alpha)}{2\left(\omega_o^2 - \omega^2\right)L}$$

hence, the solution for eq. 2.3 would be

$$i(t) = A\cos(\omega_o t) + B\sin(\omega_o t) + \frac{Id}{2} + \frac{E\omega\cos(\omega t + \alpha)}{2\left(\omega_o^2 - \omega^2\right)L}$$

(eq. 2.4)

Solving the root of i(t) would give the point where the current reaches zero and measuring the time between the current was at its maximum value and the root of Eq. 2.4 will give the value of the overlap angle

To solve A, lets take i (t) at t = 0, giving i (0) = 0

$$A + \frac{Id}{2} + \frac{E\omega\cos(\alpha)}{2\left(\omega_0^2 - \omega^2\right)L} = 0$$

$$A = \frac{E\cos(\alpha)}{2\left(\omega_0^2 - \omega^2\right)L} - \frac{Id}{2}$$

To solve B, we differentiate eq.2.4 to give

$$\frac{d}{dt}i = -A\omega_o\sin(\omega_o t) + B\omega_o\cos(\omega_o t) - \frac{E\omega^2\sin(\omega t + \alpha)}{2\left(\omega_0^2 - \omega^2\right)L}$$

(eq. 2.5)

also, from eq. 2.1, we have

$$\frac{d}{dt}i = \frac{1}{2L}\cdot(e - Vx + Vy)$$

(eq. 2.6)

equating 2.5 and 2.6 gives

$$-A\omega_o\sin(\omega_o t) + B\omega_o\cos(\omega_o t) - \frac{E\omega^2\sin(\omega t + \alpha)}{2\left(\omega_0^2 - \omega^2\right)L} = \frac{1}{2L}\cdot(e - Vx + Vy)$$

(eq. 2.7)

At t = 0, we have

$$B\omega_o - \frac{E\omega^2 \sin(\alpha)}{2\left(\omega_o^2 - \omega^2\right)L} = \frac{1}{2L} \cdot (E\sin(\alpha) - Vx + Vy)$$

hence,

$$B = \frac{E\omega^2 \sin(\alpha)}{2\omega_o\left(\omega_o^2 - \omega^2\right)L} + \frac{1}{2L\omega_o} \cdot (E\sin(\alpha) - Vx + Vy)$$

Calculation for overlap angle is shown in Mathcad in Appendix B.

2.6 Valve Stresses

It can be shown that higher d.c. currents will impose higher valve stresses. Figure 2.6 shows the valve stresses as the alpha order increases. Different current orders were also simulated to observe its effects. The CC employed in this test is 1 p.u. The characteristic of a naturally commutated converter is also included.

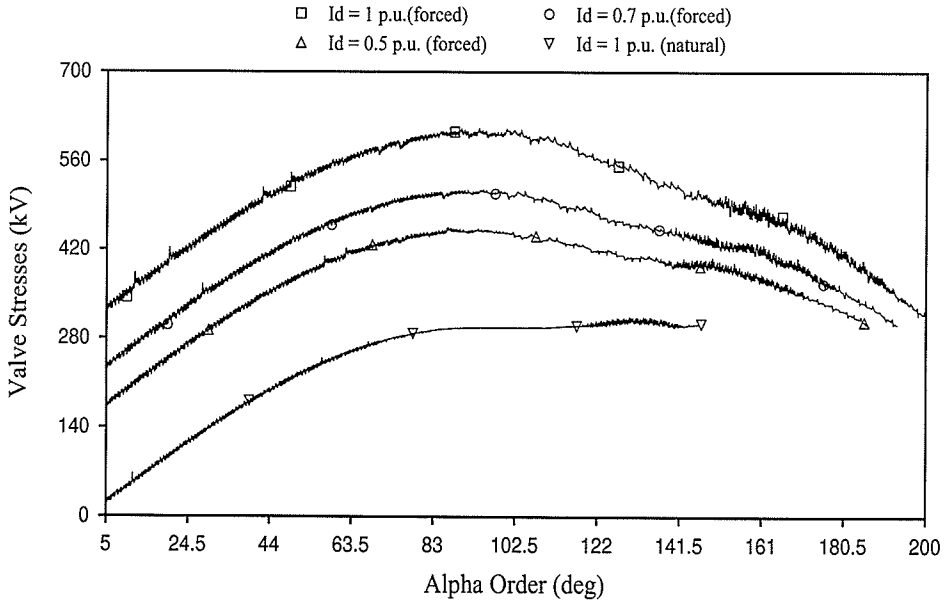

Fig 2.6 Valve Stresses with Higher Currents

We can see that for the conventional converter, operation at the normal 140 to 150 degrees will give a peak valve voltage at about 280kV. The plot also shows that the conventional converter can only be operated up to about 150 degrees before experiencing commutation failure. Also note that unlike a conventional converter, the firing angle range will be reduced for a smaller d.c. current

On the other hand, the CCC will have increased valve stresses in that operating region. For example, the same firing order for the CCC with 1 p.u. current, will impress 500kV on the valves. An increase of nearly 100% from the conventional converter due to the increase in commutation voltage.

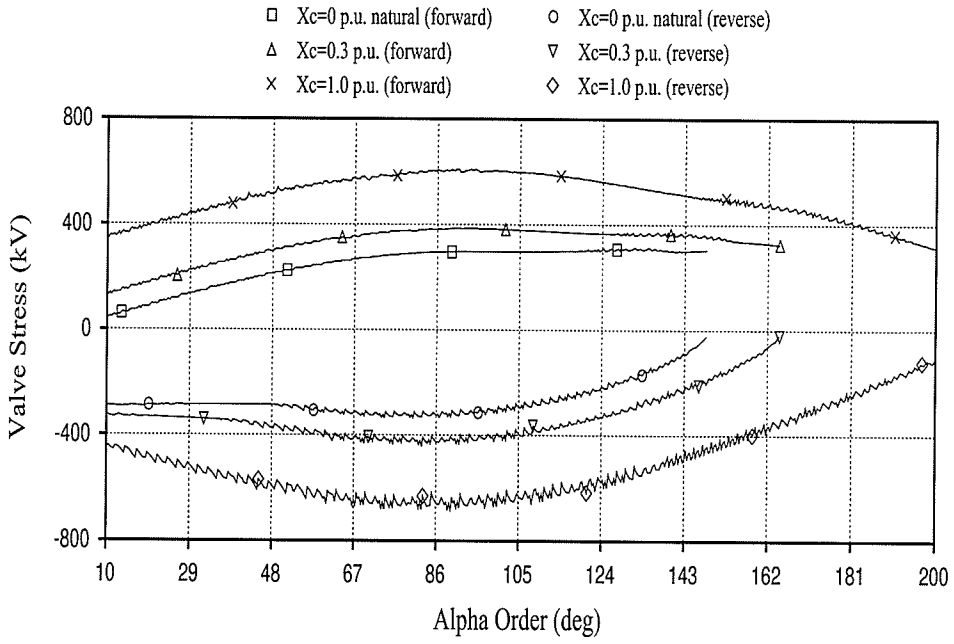

Fig 2.7 Forward and Reverse Valve Voltages with Varying X_c

Figure 2.7 above, shows the effect of varying the size of the CC. Both peak forward and reverse voltages increase with a bigger X_c but gives an increased operating range. Again, the valve stresses (for a CC of 1 p.u) at around 140 degrees alpha order would be nearly twice the conventional converter.

It is likely that the initial implementation of the CCC will be for smaller X_c and hence, a more modest control range. For example, with X_c = 0.3 p.u., we can only operate at α = 166 degrees at 1 p.u. d.c. current but maximum positive or negative valve voltage is only 30% more.

2.7 Capacitor Size Analysis

Several tests were conducted to ascertain the optimum CC size with respect to harmonics with a reduced shunt filter (Q = 0.3 instead of Q = 0.6 since the Q requirement is small). The sizes which were tested were 0.2 p.u., 0.4 p.u., 0.6 p.u., 0.8 p.u. and 1 p.u. Table 2.2 below show the results at a glance.

X_c (p.u.)	Voltage THD (%)	Gamma (degrees)
0.2	1.153	20.7
0.4	3.32	40.5
0.6	4.44	51.3
0.8	5.45	57.6
1	6.37	62.1

Table 2.1 Harmonic Content increases with X_c

Here, we can see that a higher value of X_c would cause a higher Total Harmonic Distortion, although it is very favourable to use high p.u. capacitor values for improved converter performance. This finding is consistent with the conclusion drawn by Asplund et al [3], which states that a higher X_c would result in higher harmonics because the overlap angle is reduced. Industry standards specify that THD limit should be within 2.5% of the fundamental. In this case, an acceptable CC size should be between 0.2 and 0.4 p.u. Table 2.1 above also indicates the increasing gamma with X_c.

Even with Active Filtering (which will be discussed in the next chapter), the increased harmonic generation due the larger CC would demand a higher current injection

from the Active Filter. This may interact with the HVDC controls (Section 4.3) and create instability in the system.

A large CC would also incur higher valve stresses and high $\frac{di}{dt}$ on converters [4] as we have observed in Section 2.6.

2.8 Conclusions

These findings suggest that the CCC is best employed in conjunction with active filtering (as proposed in the Concept 2000 by ABB and therefore facilitate high alpha orders) due to the fact that a substantial amount of filtering is still required without the required MVArs (though some MVArs will still be needed for operation at say 170 degrees of alpha). The basic operation of active filters will be discussed thoroughly in next chapter.

If active filters are used, this would decouple the functions of filtering and Q support, common in todays converters. However, we now need to contend with higher valve and arrester ratings and also overvoltage on the CC.

Hence, a good option is to use smaller capacitors, say 0.3 p.u, and still benefit from the increased commutation margin. The valve stresses are not as large as a 1 p.u. capacitor and will reduce costs. Maximum operating range (α order) is in between the naturally commutated converter and the CCC with a big capacitor. Reactive power compensation

can also be reduced with the slightly increased firing angle range.

CHAPTER THREE

SIMULATION COMPONENTS

This chapter will discuss the components which were built and used to simulate a full working CCC.

3.1 Extinction Angle Measurement

As mentioned earlier, the apparent (or conventionally measured) extinction angle of the CCC can be made very small and even negative with respect to the line-line voltage. The simulation was run on PSCAD-EMTDC [8], but the software does not have a real gamma measurement device for our purposes. Fortunately, it allows the creation of custom components as needed by the user. Hence, a CCC gamma measurement device was created specifically for the purpose of this thesis. The relevant waveforms were scrutinised to understand what was needed for the gamma measurement.

These were the

i) Valve firing trigger
ii) Line-line voltage
iii) Valve voltage

iv) The commutation voltage of the off going valve.

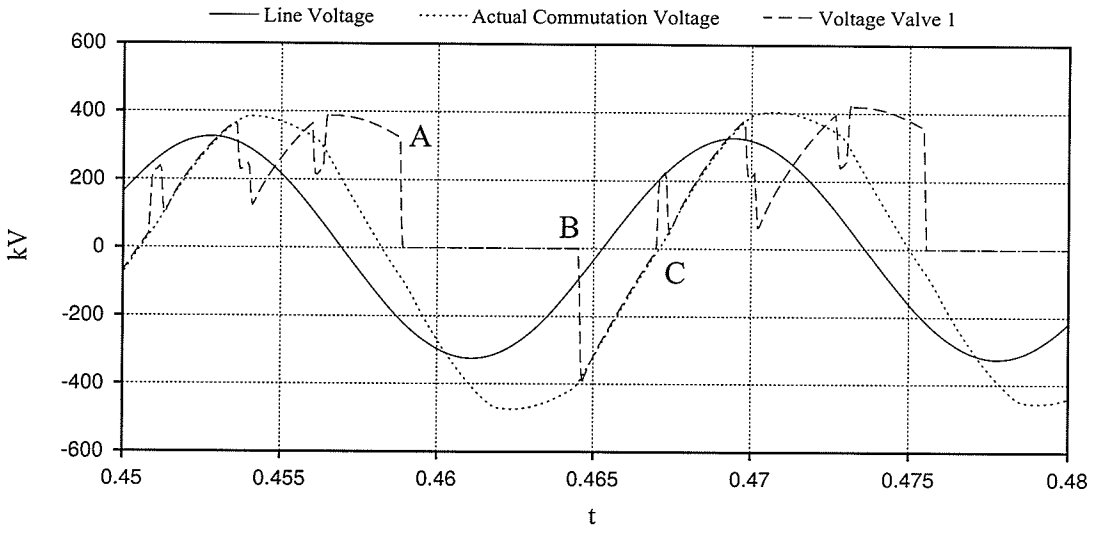

Fig 3.1 Relevant Voltage Waveforms for Gamma Measurement

From the diagram above the extinction angle measurement was initialised as soon as the firing of the valve takes place (point A on above figure). From then on, the program will start looking for negative going valve voltage. As soon as the valve voltage crosses zero to the negative region (point B), the program will memorise the zero crossing time. Next, the program will look out for a positive going commutation voltage. At the precise moment when that happens, the time is marked again (point C). The program will then have the start time and the stop time of the valve voltage in the negative region. This is then converted into angular degrees for display and further calculation/control purposes in the main EMTDC program. The block designed for this is included in Appendix C.

The component is then fed with 3 relevant waveforms from each valve (trigger signal, valve voltage and commutation voltage) via a vector component to minimise the PSCAD draft size. The definition subroutine of this component includes a minimum gamma facility to extract the most severe gamma from the valve group. This component also gives an instantaneous gamma measurement as soon as a new gamma is measured. Either real gamma or apparent gamma may be measured, depending on whether line voltage or the capacitor commutation voltage is fed into the component.

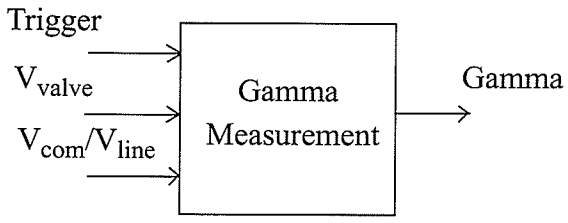

Fig 3.2 Gamma Measurement Block

The gamma measurement circuit was repeated again for the second six valve group. However, only the minimum gamma chosen from either group will be exported to the controls as it represents the worst case.

3.2 Firing Circuit

A phase locked loop was employed to follow the system voltages to determine the precise phase of the source. The phase locked loop looks at the line to line voltage of the bus and will produce a ramp which will then be compared to the turn on level (alpha

order) of a particular valve [9]. When the ramp exceeds the value of the alpha order, a firing pulse will be given for the valve (Fig 3.3). This pulse will be continuous throughout the duration that the valve is required to turn on to ensure that no premature extinction takes place although the ideal thyristor does not require a continous pulse once it is already on.

The valves were controlled as if they were GTO's, whereby a turn-off is signal is applied in the form of a negative edge at the end of the continous pulse. This negative edge is given by the oncoming valve. For example, when the ramp of T3 exceeds its turn on value at point A, its turn on signal is also passed on simultaneously to turn off T1. This procedure ensures that T1 will be pulsed for as long as possible during its required conduction period to prevent unwarranted turn off without any complications for the oncoming valve.

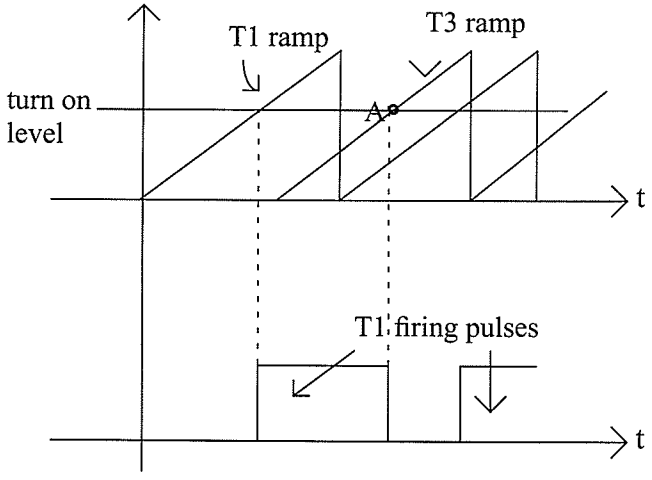

Fig 3.3 Phase Locked Loop Generating the Firing Pulses

3.3 Capacitor Voltage Imbalance Modulation

As the capacitor starts to charge up, we can observe high levels of dc components in the capacitor voltage. This high values of dc components would delay steady state operation of the circuit and needs to be damped. It would also limit the life span of the components system, especially the converter transformers. Getting the capacitor balanced is also important for control of gamma spread. It is also observed that during faults and current order changes, that these dc components would exist in the CC.

Based on the paper by Verdolin et al [10], we may control these dc values by introducing slight firing modulations on each valve in the CCC to counter the phenomenon. The modulation is based on achieving equal areas between the positive and negative areas enclosed by the capacitor voltage. We can see that the area is determined by the instant when a particular valve is fired. Let us examine Fig 3.4 below, which is the CC voltage waveform for phase A.

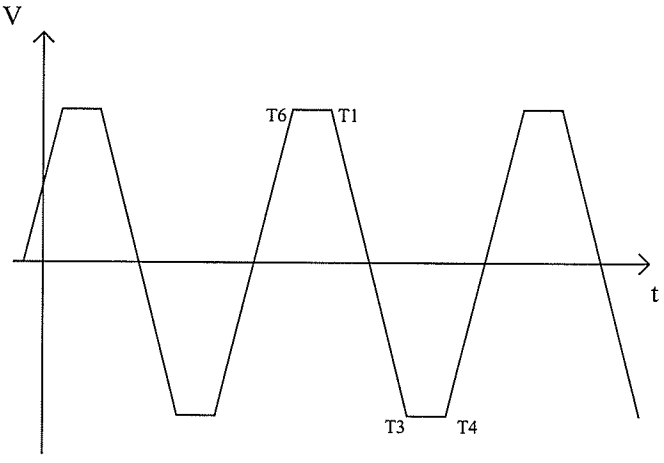

Fig 3.4 Points Modulated to Minimise DC Components

The positive half of the capacitor voltage waveform is determined by the firing of thyristors T6 and T1. Similarly, the negative half of the wave is determined by the firing of thyristors T3 and T4. To reduce the area of the positive half, the firing angle of thyristors T6 and T1 will be made earlier with respect to its alpha order to decrease the peak voltage of the capacitor and the waveform width. On the other hand, the negative area of the waveform can be made bigger by delaying the firing angle of thyristors T3 and T4. Similar analysis can be made for the other voltage components in phases B and C.

The levels of dc component in the capacitor voltage is determined by using the FFT component in PSCAD. We will then allow this reading to pass through a proportional-integral controller. The controller will give an offset with respect to the actual firing angle. A block diagram of the full firing angle modulation, is shown below in Fig 3.5.

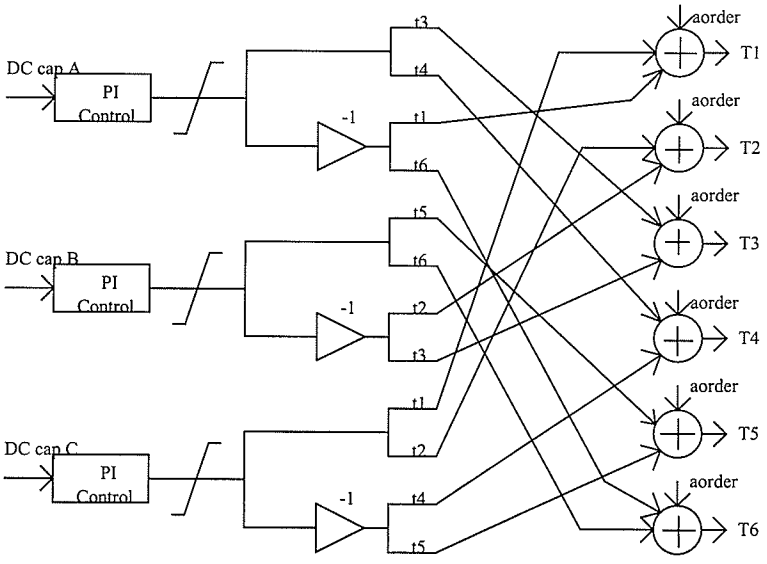

Fig 3.5 Modulation Process in Adjusting Firing Angles

Full firing angle modulation was mentioned because we could also modulate the firing angle in the 'half modulation' mode. This only makes adjustments to only two thyristor firing angles (rather than the full four points), one at the end of the positive half of the CC voltage and one at the end of the negative half of the CC. i.e. thyristor T1 and T4 only for CC voltage in phase A. From simulations it was determined that the full modulation mode is superior and hence will be used throughout this thesis. It is also shown with good result the effectiveness of these modulations in controlling the dc components with respect to a non-modulated firing control.

Figure 3.6 below shows the results of a CCC with and without modulation after a disturbance of the steady state by a change of current order from 1 p.u. to 0.5 p.u. Various proportional gains and integral gains were used to determine the optimum control parameters for modulation control. It was determined that a proportional gain of 0.05 and an integral gain 10 was satisfactory for this circuit as opposed to higher gains which would cause instability for the dc voltage and current.

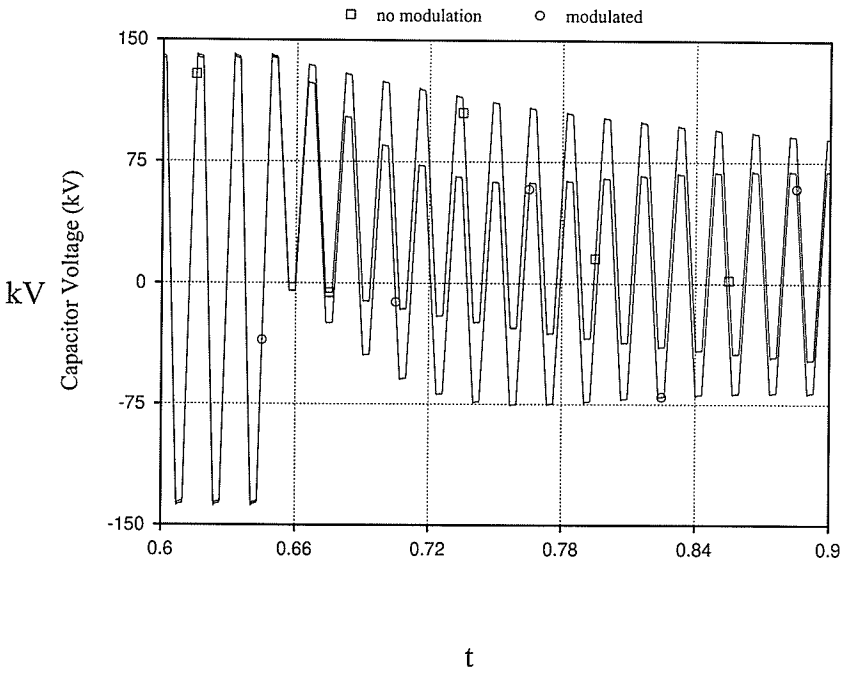

Fig 3.6 Performance of Modulation during DC Current Drop

It is shown above that the modulation works faster in restoring the d.c. values to zero in the CC. However it presents a higher dc transient during the control period depending on the value of the capacitor voltage during the disturbance and the gains used in the modulation controls. The performance of the modulation system is also shown below for the plots of dc components during start up of the system. Here, we can see that the modulation does not really help the dc components reach steady state as claimed by the authors in [4].

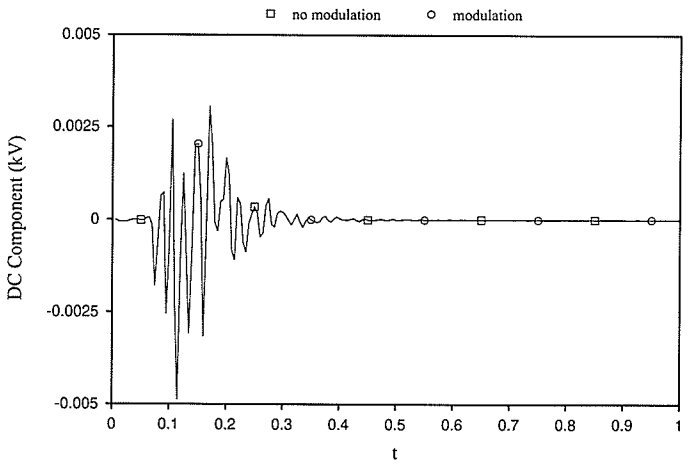

Fig 3.7 Modulation Results during Start-Up

3.4 Active Filters

The CCC allows one to operate with minimum reactive power being supplied by the ac system. However, conventional filters also supplies reactive power. If the reactive power of the filter is reduced, then the filters are more susceptible to detuning on frequency changes or effects of ageing. Hence, it was proposed [3] that active filters be used instead to cancel the harmonics whilst the minimum required reactive power was supplied via shunt capacitors.

Active filters work on the premise of introducing an opposite current waveform to the ones that it wishes to cancel. This technology in principle, is proposed in future airliners (minimising cabin noise from engine) amongst other things. Active filters are flexible due to the lack of need to tune to a particular frequency.

In HVDC applications, the 11th and 13th harmonic are predominant for the usual 12 pulse bridge configuration. Hence, the aim of the active filters in our application would be to inject an opposite harmonic current to eliminate the 11th and 13th harmonic. The exact implementation is as in the M.Sc. thesis of M. H. Abdullah (University of Manitoba, 1996). It employs a harmonic magnitude and phase detector (this was realised by using the FFT component in PSCAD) and reproduces the same harmonic current within the control circuit. This harmonic current is then inverted and for our purposes, will be called the ordered harmonic current. This value was then passed on to a current source for the ordered harmonic current to be injected into the ac system. A simple block diagram below shows the main principles of active filtering.

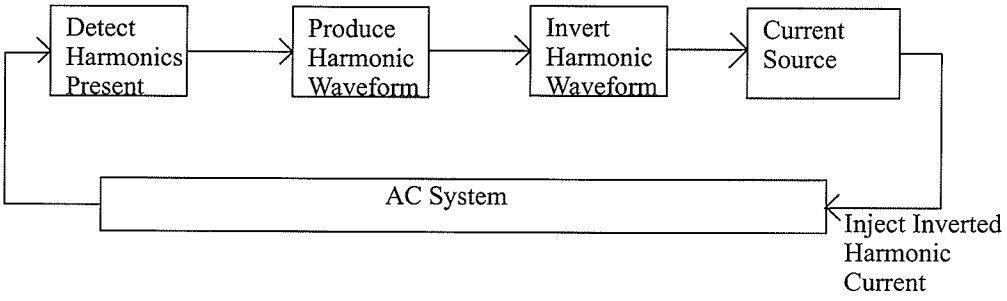

Fig 3.8 Simple Block Diagram of Active Filter Concept

The current injection was based on the Pulse Width Modulation (PWM) concept. The firing circuit is shown in Fig. 3.9. The ordered harmonic current will be the *ideal* injected current (I_{order}). However, this device (Fig 3.10)implemented a firing circuit with a voltage source and our injection cannot follow this order completely. The real injection ($I_{control}$), will attempt to follow I_{order} as best it. If $I_{control}$ is bigger than the I_{order} by a mar-

gin, it will start going down again. If $I_{control}$ is smaller than I_{order} a margin, it will start increase.

The increase/decrease of $I_{control}$ is realised with the PWM control and Figure 3.9 illustrates this fact quite clearly. The previously mentioned margin/tolerance band, is set by using the monostable elements in the firing controls. A smaller the band would lead to a more accurate imitation of the I_{order} by the $I_{control}$ but the band cannot be too small due to the high switching frequency leading to higher losses in the solid state device. The current injection into the bus is made via a passive filter, tuned to the 11th and higher order harmonics.

An alternative method to active filtering was to use the Contune concept proposed by ABB [3]. Essentially, the inductor in an LC branch can be varied with great rapidity to match the desired frequency rather than using the above proposed method.

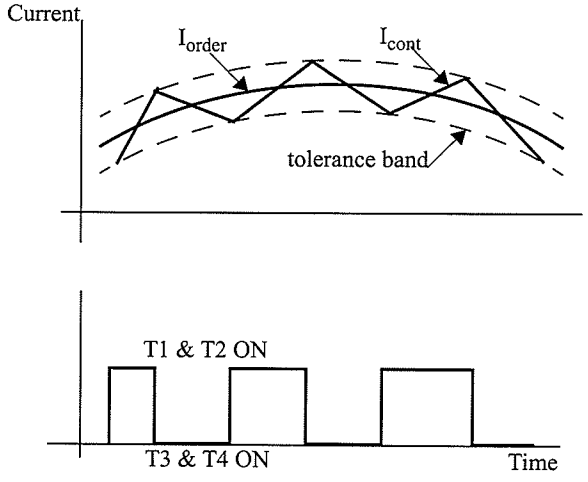

Fig 3.9 PWM Inverter Tolerance Band Switching

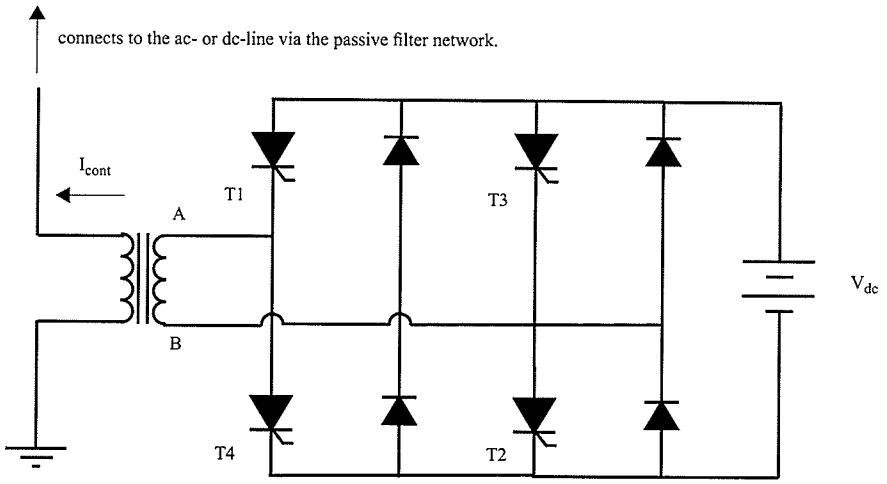

Fig 3.10 The Active Filter Firing Circuit

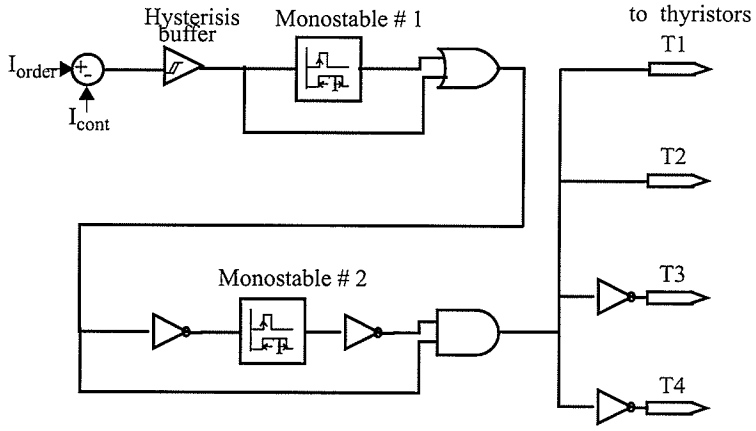

Fig. 3.11 Firing Controls Active Filter Bridge

3.5 Control of the CCC

The CCC employs the same basic control principles as the conventional converter. It has a Constant Current Control (CCurrC) for operating at reduced voltages. However, Constant Extinction Angle Control (CEA) at the inverter would not really have meaning here because $\alpha + \mu + \gamma$ does not total 180 degrees. However since CEA control essentially controls voltage, it would be replaced by Constant Voltage Controls (CVC) [8]. To maintain security, the minimum measured gamma (mentioned previously) was also monitored to ensure that it is not too small and compromise performance. Hence, Minimum Gamma Control sets the maximum alpha order limit at which the converter may operate and its alpha order only goes through to the thyristors during low readings of gamma.

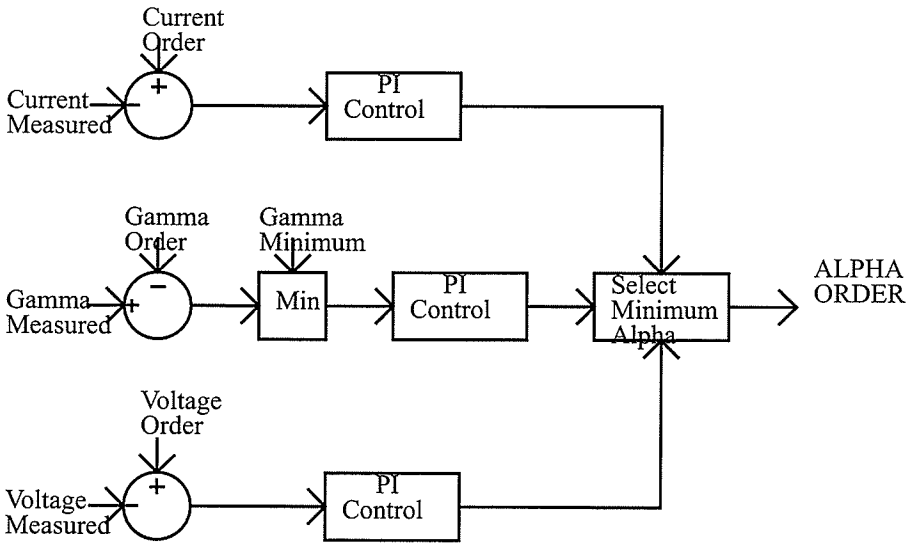

Fig 3.13 Block Diagram of CCC Firing Controls

CHAPTER FOUR

SIMULATION RESULTS

This chapter will analyse the performance of the CCC during steady state and transient periods. These tests are listed below:

i) Active Filter Observations

ii) Voltage Sag Performance

iii) Single Line to Ground Fault between Capacitor and Converter Transformer

iv) Close in Single Line to Ground Faults on AC Side

v) Capacitor Bank Outage

vi) Long Submarine Cable Performance during Single Line to Ground Faults

4.1 General Circuit Observations

The circuit must be configured differently for different size CCs. Although one would expect that the 1 p.u. CC inverter would not require reactive power consumption due to its ability to fire close to $\alpha = 180$ degrees, some shunt compensation was still supplied as it is inevitable that some reactive power will be supplied from the filters. Table

below shows a comparison of 2 sizes of CC (1 p.u. and 0.3 p.u.) with different compensation requirement and different gains to demonstrate the different requirements of different magnitudes of the CC's in systems.

	Inv Voltage ControlKp	Inv Voltage Control Ti	Rec. Curr Control Kp	Rec Curr Control Ti	High Pass filter gives
1.0 p.u	0.5	1	0.1	0.03	170 MVAr
0.3 p.u	1	0.5	0.4	0.02	125 MVAr

Table 4.1 Different Settings for CC Values

Table 4.1 above shows that for a bigger CC, the system must be treated more carefully with the controls slowed down. If the gains for the 0.3 p.u. capacitor were used for the 1 p.u. CC, instability will occur. A considerable amount of compensation is also needed for both big and small capacitors to eliminate harmonic ripple on the voltage waveform.

4.2 Filtering Requirement

A 12 pulse converter will eliminate the 5th and the 7th harmonic as the star-star and star-delta connection will each produce those harmonics at 180 degrees apart [6]. This leaves the 11th, 13th and higher order harmonics to be filtered out. However, the CCC has a different filtering requirement as opposed to a naturally commutated converter. Due to the ability of the CCC to fire at higher alpha orders, the reactive power requirement is lower. However, Asplund et al [3] have shown that the harmonic generation is in the

region of 20% greater than the conventional converter due to the reduced overlap angle. It was also observed that the higher the p.u. value of the CC, the greater the ripple magnitude. Hence, the use of passive filtering must be optimised.

This was done by the reduction of the MVAr rating of the 11th and 13th harmonic but the shunt capacitors had to be increased to cope with the higher order harmonics. Active filtering will be discussed in the next section.

4.3 Active Filter Interaction with CCC

An active filter as discussed Chapter 3 has the advantage of being able to eliminate the desired harmonics with negligible fundamental frequency reactive power supply. Discussed below are the results of the simulation.

It was observed that the Active Filter interacts with the dc components of the CCC if it samples the harmonics frequently or if it injects too much harmonic cancellation current. This happens when the active filter is abruptly turned on with the full ordered current. The interaction involved creating oscillatory dc current and voltage. This was observed to be more inherent in models which uses a big CC. Figure 4.1 below shows the introduction of the Active Filter injection to a CCC with 0.6 p.u. capacitor and how it affects the dc components. Fig 4.2 shows its effects towards the 11th harmonic content.

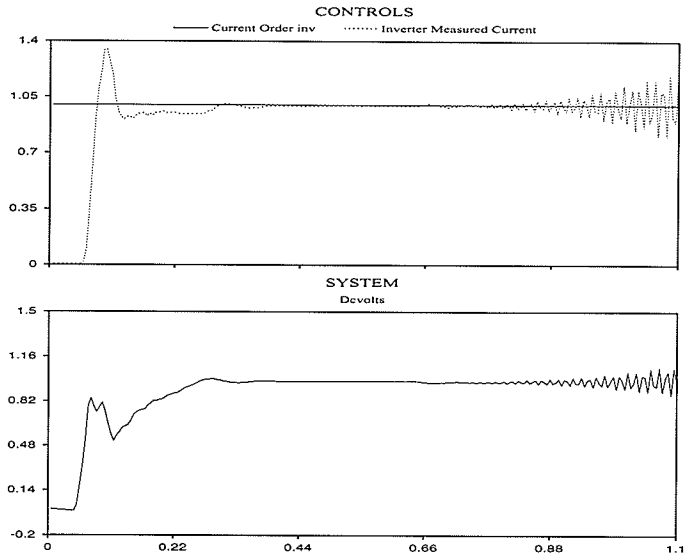

Fig. 4.1 Active Filter Injection Effects on DC Components with Abrupt Start-up for a CCC with Big Series Capacitor (1 p.u.)

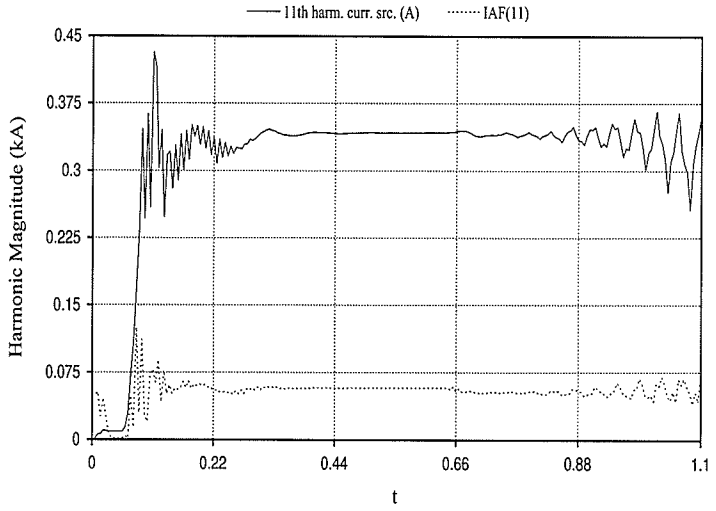

Fig. 4.2 Active Filter Injection Effects on Harmonic Manitudes with Abrupt Start-up for a CCC with Big Series Capacitor (1 p.u.)

To counter these oscillatory components, the active filter was turned on slowly by increasing the injection current from a low value to the actual needed value. Further, the sampling frequency must be low to prevent the active filter from over reacting.

The plot above also shows that the active filter can even increase the harmonic content if the Active Filter injection is not exactly the opposite of the harmonic current. Hence, the active filter controls play an important part in eliminating harmonics and also maintaining system stability.

For example, the active filter current order (I_{order}) can be generated by 2 different algorithms. The first algorithm looks at the current coming out from the converter ($I_{original}$), processes the current reading and generates the 11th and 13th harmonic through an FFT component. This 11th/13th current will be inverted (I_{order}) and injected back into the ac system via a current source. This method only eliminates the 11th and 13th harmonic.

The second method will still observe the current $I_{original}$ from the converter but instead of generating the 11th and 13th harmonic through the FFT component as before, it will generate the fundamental current (I_{fund}) instead. This current will then subtract $I_{original}$ and the result is inverted to become I_{order}. This method eliminates all harmonics. The simplified Figure 4.3 below illustrates this method.

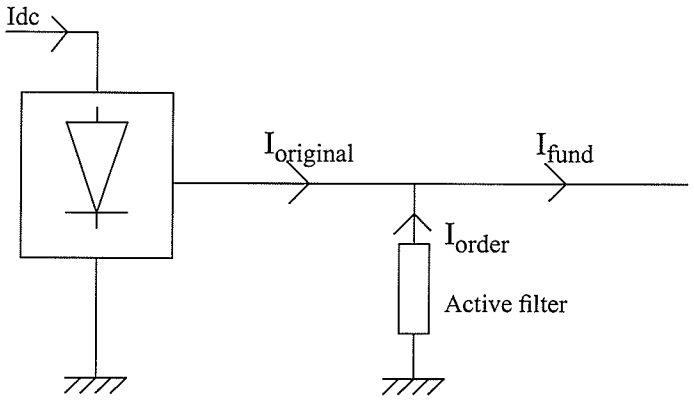

Fig. 4.3 Currents for Active Filtering

Since we have generated I_{fund} through the FFT, and know $I_{original}$, we can determine that $I_{order} = I_{fund} - I_{original}$.

Tests were done using both methods. Theoretically both methods would be effective in eliminating the dominant harmonics (the 11th and 13th). It was observed that the second method was more stable as the first method creates oscillation almost immediately after it was turned on. This may indicate that the I_{order} from the first method may interact with the inverter controls and cause the oscillation.

Active filtering was supported with passive shunt filters to limit high frequency ripple. If the high frequency were to be left for the active filter to suppress, its injection to the system would be too great and the system would become unstable, even for systems with small CCs.

Another observation was that the Active Filters should be turned on only after the system has reached steady state. This was due to the inconsistent harmonic content which exist during the start up transient might order the wrong magnitude of required injection.

4.4 Voltage Sag Performance

Voltage sag would reduce the ability of the line voltage to commutate valves in a conventional converter. The same would be true for the CCC but because it has an additional commutation voltage, the likelihood of a commutation failure is reduced. Fig. 4.4 below show the DC components during the period of voltage sag. In this case, the ac source voltage was reduced by 10% from 217 kV to 195 kV. The CC size was 0.3 p.u.

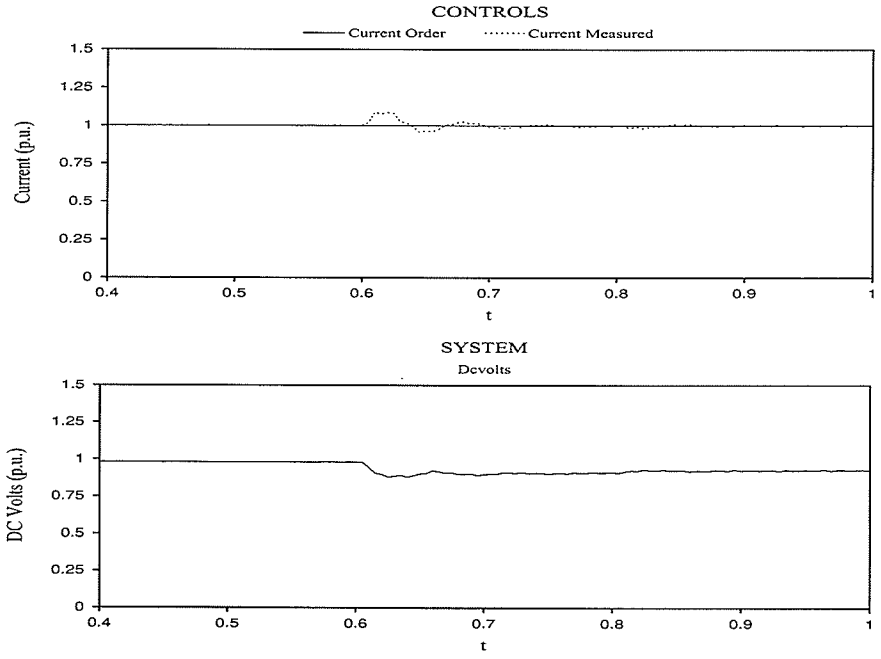

Fig 4.4 DC Components during Voltage Sag

We can see that the dc current oscillates slightly at the introduction of the sag. DC voltage dropped to 0.8 p.u and will climb back to it original value of 0.98 p.u. by increasing the alpha order. However, the gamma control (Section 3.5) limited the dc voltage to 0.92 p.u due to security reasons as higher alpha orders would make the extinction angle too small.

A test on the conventional converter showed that voltage sag of 7% can cause commutation failure. The CCC can withstand 10% and still be operational with no prior commutation failure. The 10% voltage sag value was chosen as it represents the worst case scenario in the Tenaga Nasional Berhad, Malaysia grid.

Therefore, commutation failure performance is improved by giving the CCC immunity up to a certain extent against a low line voltage. If the ac system voltage would drop more than 10%, frequency drop would ensue and other machines in the grid would trip. Hence, immunising the CCC for more than 10% voltage sag would not be very useful because the ac system has already collapsed. However, power transfer of the inverter will be reduced due to the lower allowable dc voltage, as limited by the gamma controller. This is due to the tendency of the voltage control to fire at a higher alpha order to compensate for the lower dc voltage due to the ac voltage sag.

The gamma controller will limit the firing angle to ensure that there is still enough commutation angle for the outgoing valve to turn off. Although it is not operationally practical, tests have shown that in this particular case, the CCC can continue operation

even with a 35% voltage sag at a reduced power transfer of 0.7 p.u. This demonstrates the immunity of the CCC with respect to voltage sag.

4.5 AC Faults on Inverter Side

4.5.1 Single Line to Ground Fault between Capacitor and Converter Transformer

A fault between the CC and the converter transformer showed good results with the CC limiting the fault current through the valves. Figure 4.5 shows the path of the fault current. In the case below, the dc line was modelled as a cable, length 400km, nominal dc voltage at 500kV, dc current at 2kA.

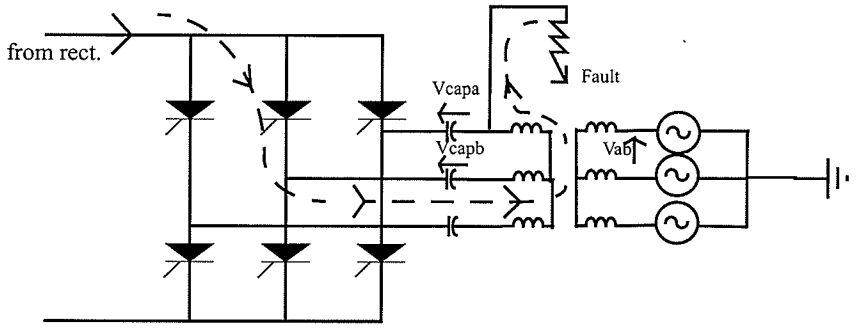

Fig. 4.5 Discharge Path of DC Line for a Fault between the CC and the Transformer

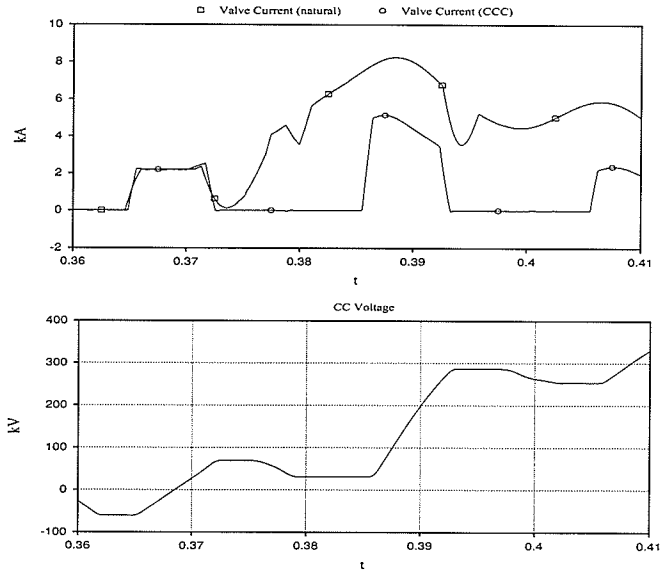

Fig 4.6 Fault Current Limited in the CCC

Fig. 4.6 shows the most severe valve current in the fault mentioned in the previous page. The presence of the capacitors can be seen to limit the fault current by half as compared to the performance of the conventional converter. As the fault current increases due to the discharge of the dc line, the CC voltage increases. This creates a counter voltage to the fault current and reduces the fault current significantly. This characteristic is especially useful to counter large discharge currents from a long cable with a big capacitance.

It is assumed that the fault is cleared after 2 cycles (i.e. at t = 0.41s) and the CC voltage will rise no further. It is recommended that the CC and to be rated at the maximum voltage it might endure within 2 cycles to maintain its counter voltage capability during the fault. The varistors protecting the CC, may be rated slightly higher.

4.5.2 Close In Single Line to Ground Fault on AC Side

Single line to ground faults were simulated. There is still some load rejection over-voltage because of the necessity of the high pass filtering capacitors. Overvoltages for CC were also noted for design purposes. All figures Table 4.2 are in p.u. unless otherwise stated.

CC size	Peak AC Voltage (on recovery)	Original CC Voltage (kV)	Peak CC Voltage (kV)
1.0	1.29	227	456
0.6	1.24	125	289
0.3	1.20	61	161

Table 4.2 Single Line to Ground Fault Values

The conventional inverter dc currents and voltages did not exceed 1 p.u. during the fault. Its ac overvoltage however was 1.5 p.u., higher than the CCC. We can conclude that the CCC does reduce the overvoltage rejection ratio but not considerably as the author would have hoped due to the high pass filters. The CCC is also immune against ac side faults with an X_c greater than 0.88 p.u. Recovery times are comparable to the conventional converter.

Arrestors may be used to protect the converter capacitors. In this case, a 120kV arrestor was used for the 0.3 p.u. capacitor. Instead of the capacitor voltage going all the way up to 161 kV, the arrestor will conduct and protect the capacitor. However, tests show that

this limits the counter voltage capability of the capacitor, and results in a higher valve current (by 1 kA in this case).

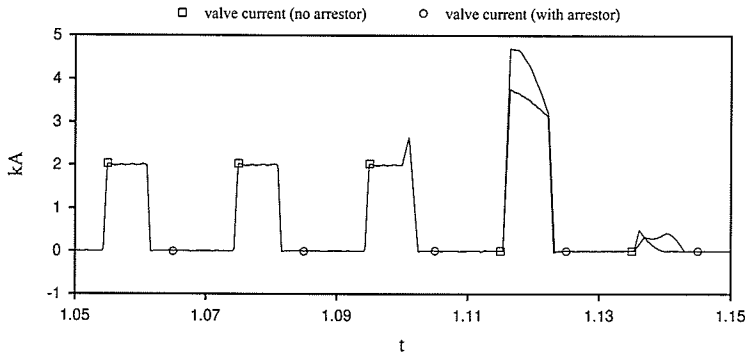

Fig 4.7 Increased Valve Current with Arrestor Implementation

4.6 Capacitor Bank Outage

Each CC in each phase is made up of several branches of parallel capacitors to make up the value and rating of the CC. For instance for a 6 pulse valve bridge, with a 500 MW converter transformer and a 120uF CC, each phase will carry about 170 MW. However, the capacitors are rated with respect to its 'throughput', i.e. I^2Z will give about 66MVA for each CC.

However, due to the possibility of a capacitor bank outage (e.g. one of the parallel capacitor breaks down) the remaining parallel capacitors will have to be rated to compensate for the increase in power rating. Figure 4.8 below shows the CC arrangement for one phase, comprising of 6 parallel capacitors. Further, a loss of a single bank will still allow

the CCC to continue operation as will be shown in Fig 4.5. It must be noted that this arrangement is an exaggerated simplification for simulation purposes only. Industry capacitor arrangements are usually done in a mesh. So for a CC of 66 MVA rating, we may need 100 capacitor cans, as the biggest capacitor in the industry presently is rated at about 700kVA.

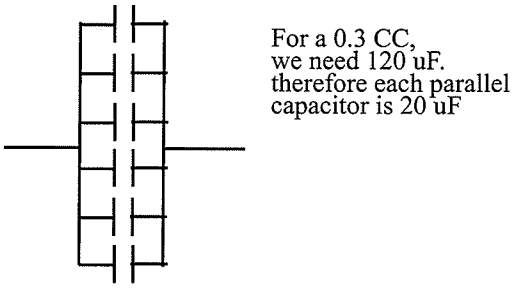

Fig 4.8 6 Parallel Capacitors Making Up a 0.3 p.u.CC for 1 Phase

Capacitor bank outage simulation is based on the above figure. The results are plotted in Fig. 4.9.

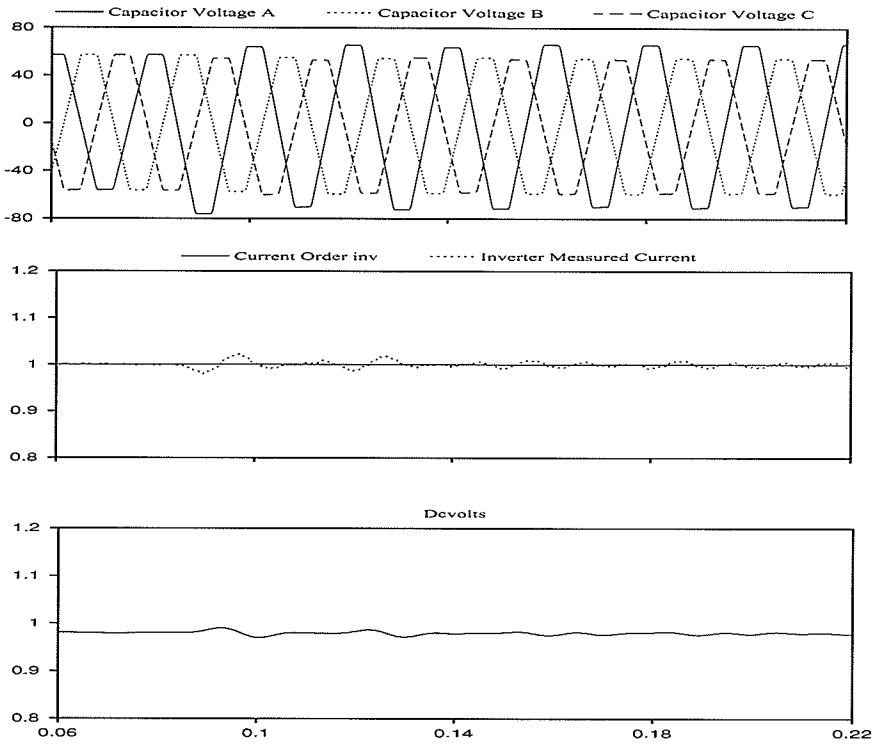

Fig 4.9 DC Component and CC Voltage after Loss of 1 Bank in Phase A Y-Y Group

Fig. 4.9 above shows that for a 0.3 p.u. CC, the CCC can still maintain operation after the initial 1 bank outage and can go on indefinitely. The combined impedance of phase A CC is now higher, as it has a smaller uF value. It was observed that gamma for phase A also increases from 27.4 degrees to 30.1 degrees due to the bigger new X_c p.u. value. Phase A CC voltage is almost transient free, demonstrating that the dc modulation/ balancing circuit is effective in damping any dc components after a disturbance.

The minimum gamma reading of the whole valve system is reduced (from 27 to 26.5 degrees)due to the fact that alpha order is higher to compensate for the new quasi steady state small oscillations in the dc voltage. AC line voltage stays at the same value as before the bank outage. Harmonic values are practically the same as before as well. Valve over-voltages do not occur due to loss of capacitor banks if the system continues operation.

Simulations on increased bank outage were also done to check on system stability and also overvoltages. Below is a tabulation of the results.

Bank Outage	**Peak CC Voltage on Remaining Parallel Capacitors**	**Peak Valve Voltage**
1 of 6	1.2 p.u.	1.03 p.u.
2 of 6	1.5 p.u	1.17 p.u.
3 of 6	2.68 p.u	1.35 p.u.

Table 4.3 CC Outage and Valve Overvoltages

It is therefore shown that a higher fraction of bank outage versus the remaining banks will result in higher overvoltages. This would imply that the greater the number of parallel connections, the less perturbed the system is (based on the same number of bank outage). However, increasing the number of parallel capacitors would also increase cost. That number must therefore be based on the expected number of bank failures, valve ratings, cost of the capacitors and its auxiliary equipment and insulation coordination. Also,

for the remaining capacitors to stay operational after bank outages, they must be rated to share the power that was carried by the faulted capacitor/capacitors before the outage.

An interesting possibility which may be somewhat impractical at this stage would be to connect a spare capacitor bank back into the parallel configuration. Each phase would ideally have a spare capacitor for each parallel capacitor but this is not economically feasible. Depending on the requirement of the system, i.e. how reliable the system should be, the amount of spare parallel capacitors can be determined. The plots below (Fig 4.10) shows the reconnection of 3 spare parallel capacitors banks at different CC voltage conditions. The vertical voltage lines in the diagram denotes the instant the spares are switched in and voltage falls to zero and the spare capacitor starts charging from then on. It appears that the spare parallel capacitors can be connected into the system at any time without any detrimental effect. However, it should be done as soon as possible after the fault to minimise the overvoltage on the CC and its dc components.

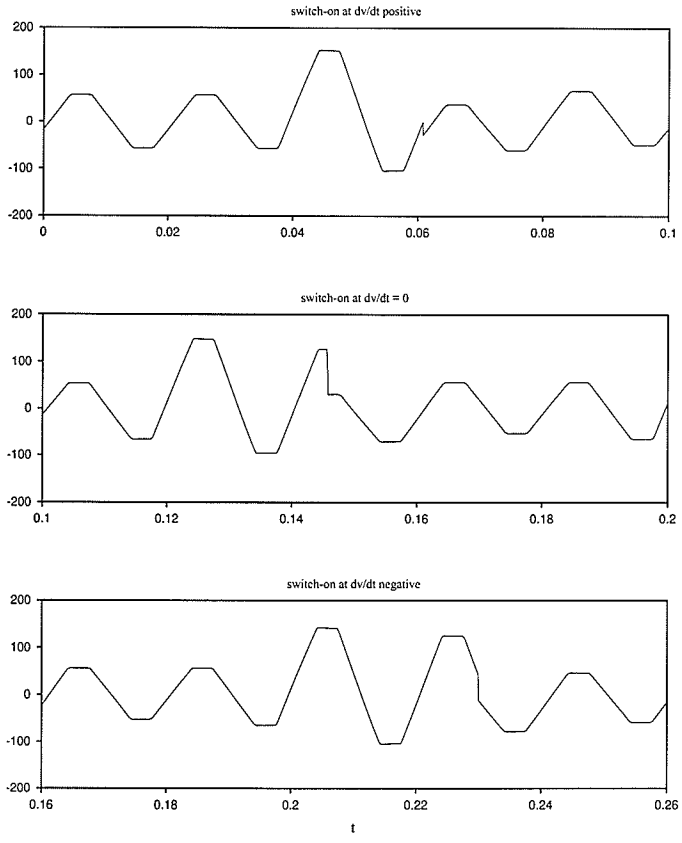

Fig 4.10 Connection of Spare Capacitor Banks into the System at Different Instances

4.7 Long Submarine Cable Performance of the CCC

As mentioned in Chapter 1, the CCC may prove advantageous in a scheme whereby a long dc submarine cable is employed. This is because a long submarine cable has a high capacitance and will store a lot of charge. If there is a fault on the inverter side, and commutation failure occurs, the very high current discharge from the cable may prevent the dc

system from recovering. Another problem is the high value of valve currents from discharge of the cable. This was discussed extensively by Karlsson and Liss [1].

To simulate the behaviour of a CCC with a long cable (the Cable Option in EMTDC was used with references to the Baltic Cable [12]) with respect to system recovery, a single line fault was applied on the inverter ac side. The cable was 500km long and the dc voltage and currents are similar to the test in Section 4.5.1. The PSCAD program option allows the simulated cable to be sheathed and armoured. The sheath is grounded to maintain a constant uniform electric field in the cable dielectric to enhance cable life. The armour is also grounded.

The fault was simulated on the ac bus of the inverter and caused a commutation failure which allowed the discharge of the cable. The rectifier and its control cannot do anything to prevent the discharge of the cable. In fact, the rectifier is effectively decoupled from the inverter. This phenomenon indicates the negative resistance characteristics of the inverter as seen from the dc side if there is no fast voltage control in the ac network close to the inverter. However, as argued in Chapter 1 as well, the CCC will increase the positive impedance characteristics of the inverter [4]. This translates into a counter voltage by the CC to limit the discharge current. A 0.3 p.u. CC was implemented in the circuit and the effect of this is illustrated below.

The test plots (Fig. 4.11) show that during the fault, the inverter dc current increased dramatically although the rectifier was not pushing any more significant current into the

dc cable. This extra current was the built up charge previously mentioned. The CCC will limit the over current to 4.05 p.u. with respect to 4.35 p.u of the conventional converter (in this case, 1 p.u. = 2kA). The rationale behind this is indicated by the CC counter voltage which increases to about 115kV, slightly more than double its steady state peak value.

Rectifier measured current did not drop to zero during the fault, indicating that the rectifier is charging the cable after the initial transient as the inverter current is zero. Force reard on the rectifier side was not simulated and hence the current is limited at 0.3 p.u. because of the Voltage Dependant Current Order Limit (VDCL) is in effect [7]. Recovery periods are comparable between the CCC and the naturally commutated converter.

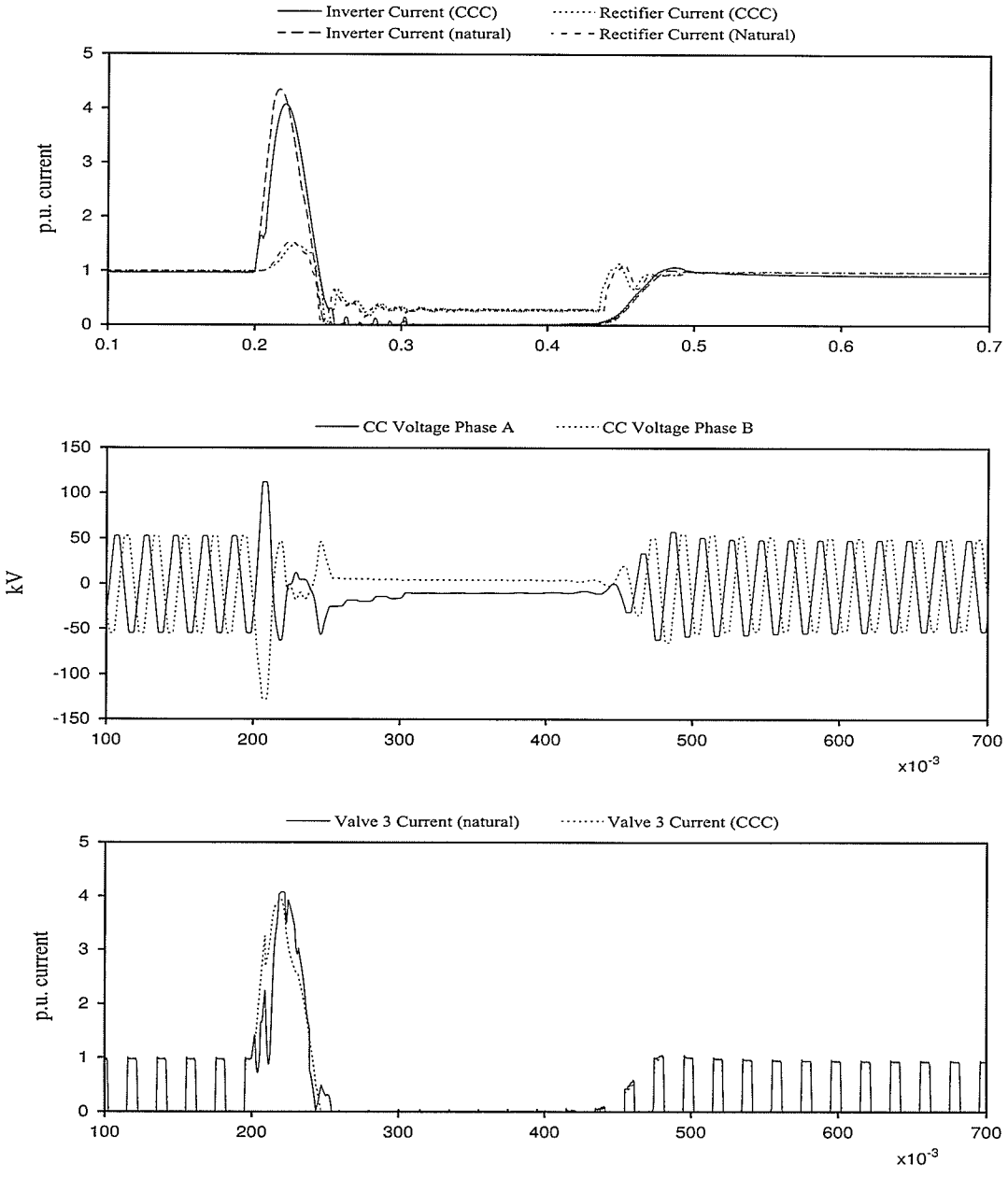

Fig 4.11 System with Long Cable Recovers from Inverter AC Fault

4.8 Test Conclusions

Several tests were made in this chapter to compare the performance of the CCC to the conventional converter.

The use of large CC's were not practical as it would demand a higher valve rating (as discussed in Chapter 2). It is also not practical as it would induce high frequency ripples on the voltage waveform which can only be filtered by large shunt capacitors. This effectively defeats the purpose of having Active Filters. Further, large CC's will reduce system agility as it uses low gains to maintain stability.

The CCC is not affected at all with a voltage sag of 10% and can withstand an even lower ac voltage. Ample gamma would still be available if the controller does not decide to increase the firing angle to keep dc voltage at 0.98 p.u.

Single line to ground recovery performance for an inverter with an overhead dc line is comparable to conventional converters. However, the valves will not experience commutation failure at X_c greater than 0.88 p.u. Further, load rejection overvoltage is reduced with the introduction of Active Filters.

Capacitor bank outage is not critical unless a large number of parallel capacitors making up the single phase CC, fails. CC reliability will be enhanced with a greater number of parallel capacitors at the expense of greater costs.

Long submarine cable application will benefit with the introduction of CC to limit the discharge of the line especially if the fault is between the valves and the converter transformer by limiting the discharge current from 4 p.u. to 2.4 p.u. For faults on the ac bus, the advantage is not very significant as the CCC only limits the overcurrent to 4.05 p.u. with respect to 4.35 p.u. in the conventional converter. Recovery takes place almost immediately after the fault is cleared. Inverter stability was also observed to improve as the same gains (on the CCC) used on a conventional converter will induce instability.

CHAPTER FIVE

CONCLUSIONS

This thesis has covered the major operational aspects of the Capacitor Commutated Converter (CCC) scheme. Chapter One has introduced the reader to the possibilities of operation with CCC. It has also shown the basic operation with increased commutation voltages available from the series capacitor. It was also mentioned that the CCC would be more stable than a conventional converter especially for long submarine cable applications due to its positive impedance characteristics and the increased commutation margin. Chapter Two has demonstrated that theoretically, the CCC may be operated at firing angles of close or even beyond 180 degrees. This is due to the significant increase of the commutation angle.

Further, a greater firing angle would also minimise reactive power requirement of the HVDC system. Several equations were also presented to calculate mean dc voltage and also the overlap angle. Increasing converter capacitors values would also increase the valve stresses. It was observed that an X_c of 1 p.u. nearly doubles the valve ratings at α = 140 degrees. Although we might not operate the inverter at that angle (as it has been

shown that we can actually give an alpha order higher than that), the valves nevertheless must be rated at the maximum simulated/calculated stresses. Further, the valve voltage stresses will also increase as a function of dc current.

Capacitor size analysis was carried out. The commutation margin increases with Converter Capacitor (CC) size. Large converter capacitors would entail larger high frequency ripple on the ac voltage due to the charging and discharging of the capacitors. Converters with large CC's were found to require less reactive power support than converters with smaller CC's due to the higher allowable firing angle and the CC's own reactive power. However, converters with larger CC will impress higher voltage stresses on the valves.

Several different component models had to be created for the computer study of the CCC. This thesis has shown the design and implementation of a gamma measurement block for PSCAD-EMTDC use. The firing circuit was synchronised with the appropriate line voltages through the use of a phase locked loop. Since the series capacitors may experience some dc components during transients, a modulated firing system was employed to expedite the decay of these dc components. All of the above has been shown to work well with the CCC.

Active filters were used in the modelling. However, the injected currents into the ac bus affects the HVDC system and the dc voltage and current were observed to oscillate with a certain choice of active filter controller. This suggests that the controls of the active

filters and the CCC must be made compatible to ensure stable operation. The active filter sampling frequency must also be reduced. Having said that, the active filters worked extremely well in cancelling the generated harmonics.

The previous chapter stated that passive filtering would still be needed to take care of the high frequency ripples as the active filters will tend to over react (and starts affecting the dc voltage and current) if left to cancel all the harmonics from the CCC on its own. Voltage sag immunity down to 10% (a typical value of voltage sag in the Malaysian Grid System) is also achievable with a 0.3 p.u. CC.

It appears that even with the CCC, we require a certain amount of capacitance for filtering the higher frequencies. This automatically introduces reactive power to the system. However, this capacitance is reduced from the value required in the conventional converter. Hence , load rejection overvoltage is reduced with the CCC due to the reduced passive filtering.

For a dc cable system, the CCC demonstrated that it can limit commutation failure because the cable discharge current is reduced by the CC counter voltage. Capacitor bank outage has no detrimental effect on the HVDC system as long as the number of parallel capacitor bank outage does not exceed a critical limit. For the simulated system in this thesis, the bank outage should not exceed 3 banks out of 6. Even then, the remaining capacitor banks should be rated to carry twice the power to be able to continue operation.

Connection of spare capacitors to replace the faulted banks theoretically can be made at any time without stopping operation.

Further work on the subject can be made to determine the actual costs of constructing the CCC converter due to the savings in filtering requirement and the increased cost in valve ratings. Investigation of the interaction between the active filters and the CCC would also be very useful.

Overall, the CCC concept is very promising. It offers better commutation failure immunity, better stability and lower valve overcurrents for certain faults in long dc cable schemes. The only drawback is that it may increase converter costs. However, the increase in converter costs is somewhat offset by the decrease in the cost of reactive power supply and passive filters.

On another note, the CCC has not been utilised anywhere and does not have a track record. This fact alone would induce reluctance of utilities to implement this idea. Hopefully, utilities will appreciate the feasibility of the scheme and take advantage of benefits which inherently comes with putting series capacitors between the valves and the converter transformer.

Appendix A

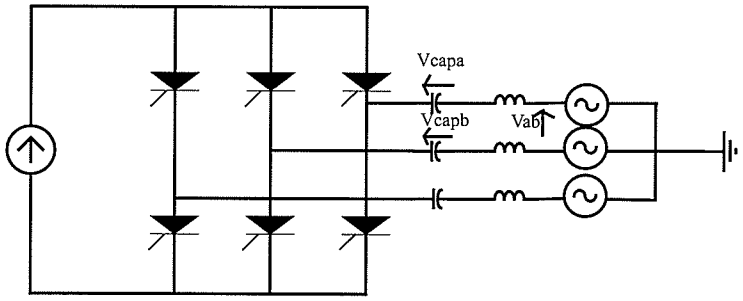

AC Source = 218kV

Primary Line - line Voltage = 230kv

DC Voltage = 500kV

DC Current = 2kA

Series Capacitor Xc = 0.3 p.u or 117.5 uF

Transformer Leakage = 14%

Transformer Secondary Voltage = 207.115 kV

Appendix B

Overlap, Extinction Angle and DC Voltage Calculations

The next few pages contain the above calculations using Mathcad as derived with assistance from A M Gole.

CALCULATION OF CCC PERFORMANCE

CONSTANTS

$TMVA = 585.1$ $VS = 207.115$ $Xc = \frac{VS^2}{TMVA}\cdot 0.14$ $\omega = 376.991$

$C = 120\cdot\mu F$ $L = \frac{Xc}{\omega}$ $\omega o = \frac{1}{\sqrt{L\cdot C}}$ $Id = 2\cdot kA$ $Vll = VS$

$\alpha = 120\cdot deg$ $\omega o = 553.241$ $E = \sqrt{2}\cdot Vll$

$$A(\alpha) = -\frac{Id}{2} + \frac{E\cdot\omega\cdot\cos(\alpha)}{2\cdot\left(\omega^2 - \omega o^2\right)\cdot L}$$

$$Bo = E\cdot\frac{\omega^2}{\omega o}\cdot\frac{\sin(\alpha)}{2\cdot\left(\omega o^2 - \omega^2\right)\cdot L} + \frac{1}{2\cdot\omega o\cdot L}\cdot\left(E\cdot\sin(\alpha) - 4\cdot\frac{Id\cdot\pi}{3\cdot\omega\cdot C}\right)$$

Basic Equations for Overlap Angle

initial estimates

$B = Bo$ $\mu = 0\cdot deg$

Given

$$A(\alpha)\cdot\cos\left(\frac{\omega o}{\omega}\cdot\mu\right) + B\cdot\sin\left(\frac{\omega o}{\omega}\cdot\mu\right) - \frac{Id}{2} + \frac{E\cdot\omega\cdot\cos(\alpha + \mu)}{2\cdot\left(\omega o^2 - \omega^2\right)\cdot L} = 0$$

$$B - E\cdot\frac{\omega^2}{\omega o}\cdot\frac{\sin(\alpha)}{2\cdot\left(\omega o^2 - \omega^2\right)\cdot L} - \frac{1}{2\cdot\omega o\cdot L}\cdot\left[E\cdot\sin(\alpha) + \frac{Id}{\omega\cdot C}\cdot\left(\frac{2\cdot\pi}{3} - \frac{\mu}{2}\right) - \ldots\right.$$
$$\left. + \frac{A(\alpha)}{\omega o\cdot C}\cdot\sin\left(\frac{\omega o}{\omega}\cdot\mu\right) - \frac{B}{\omega o\cdot C}\cdot\left(\cos\left(\frac{\omega o}{\omega}\cdot\mu\right) - 1\right)\right] \ldots = 0$$
$$+ \frac{E\cdot(\sin(\alpha) - \sin(\alpha + \mu))\cdot\omega o}{2\cdot\left(\omega o^2 - \omega^2\right)\cdot 2\cdot L}$$

$X(\alpha) := \text{Find}(\mu, B)$ $X(120\cdot deg) = \begin{pmatrix} 0.123 \\ 18.704 \end{pmatrix}$

$\mu(x) := X(x)_0$ $B(x) := X(x)_1$

$\mu(120\cdot deg) = 7.025\cdot deg$

$\alpha := 20 \cdot deg, 21 \cdot deg .. 166 \cdot deg$

Overlap

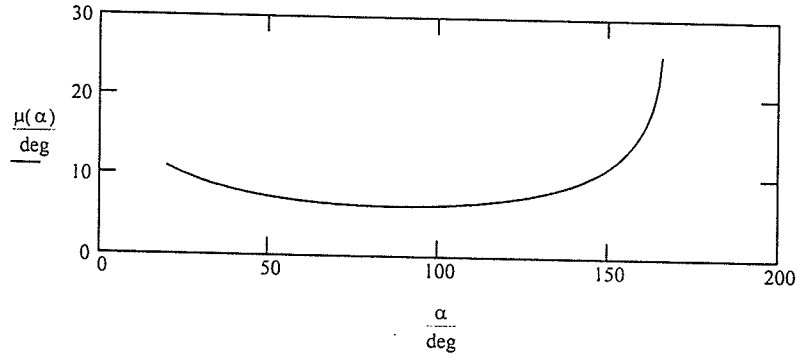

$\delta := 20 \cdot deg$

$\alpha := 120 \cdot deg$

Calculation of true and apparent γ:

$$\Delta Vx(\alpha) := \frac{1}{\omega o \cdot C}\cdot\left[A(\alpha)\cdot\sin\left(\frac{\omega o}{\omega}\cdot\mu(\alpha)\right) - B(\alpha)\cdot\left(\cos\left(\frac{\omega o}{\omega}\cdot\mu(\alpha)\right) - 1\right)\right] + \frac{Id\cdot\mu(\alpha)}{2\cdot\omega\cdot C} \ldots$$
$$+ E\cdot\frac{\sin(\alpha + \mu(\alpha)) - \sin(\alpha)}{2\cdot L\cdot C\cdot\left(\omega o^2 - \omega^2\right)}$$

Given

$$-2\cdot\pi\cdot\frac{Id}{3\cdot\omega\cdot C} + \Delta Vx(\alpha) + \frac{Id}{\omega\cdot C}\cdot(\delta - \mu(\alpha)) - E\cdot\sin(\alpha - \delta) = 0$$

(The angle δ is the time to reverse bias from the start of the commutation process).

$\delta(\alpha) := \text{Find}(\delta)$

$\gamma(\alpha) := \delta(\alpha) - \mu(\alpha)$

$\gamma app(\alpha) \quad 180 \cdot deg - (\alpha - \mu(\alpha))$

δ and overlap

$\alpha := 140 \cdot deg, 141 \cdot deg .. 166 \cdot deg$

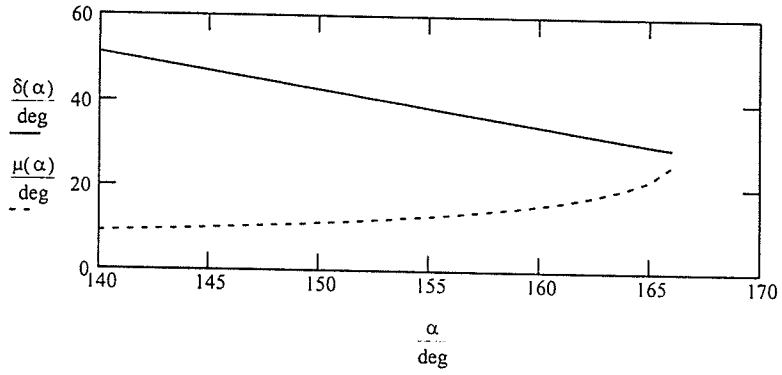

Actual and apparent extinction angle

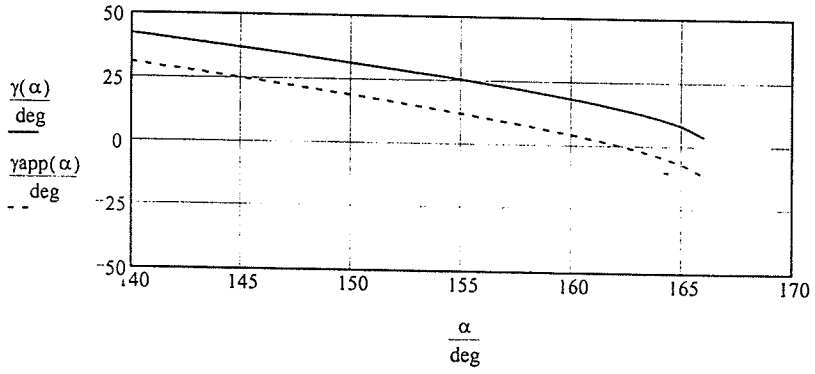

Calculation of DC Voltage

There are 3 components:

Conventional Component:

$$Vd1(\alpha) := \frac{3\cdot\sqrt{2}}{\pi}\cdot Vll\cdot\cos(\alpha) - \frac{3}{\pi}\cdot\omega\cdot L\cdot Id$$

Capacitor component during overlap

$$Vd2(\alpha) := \frac{3}{\pi}\cdot\left[\frac{\mu(\alpha)\cdot Id}{\omega\cdot C}\cdot\left(\frac{\pi}{3}-\mu(\alpha)\right)+\frac{1}{\omega o^2\cdot C}\cdot\left[B(\alpha)\cdot\sin\left(\frac{\omega o}{\omega}\cdot\mu(\alpha)\right)+A(\alpha)\cdot\left(\cos\left(\frac{\omega o}{\omega}\cdot\mu(\alpha)\right)-1\right)\right]\ldots\right.$$
$$\left.+\frac{-B(\alpha)\cdot\mu(\alpha)}{\omega o\cdot C}\quad E\cdot\frac{\omega o^2}{\left(\omega o^2-\omega^2\right)\cdot 2}\cdot(\cos(\alpha)-\cos(\alpha-\mu(\alpha))-\mu(\alpha)\cdot\sin(\alpha))\right]$$

Capacitor component after overlap

$$Vd3(\alpha) := \frac{3}{\pi}\cdot\left[\left(\Delta Vx(\alpha)-\frac{\pi\cdot Id}{3\cdot\omega\cdot C}\right)\cdot\left(\mu(\alpha)-\frac{2\cdot\pi}{3}\right)-\frac{Id}{\omega\cdot C}\cdot\left(2\cdot\frac{\pi^2}{9}-\frac{2\cdot\pi\cdot\mu(\alpha)}{3}+\frac{\mu(\alpha)^2}{2}\right)\right]$$

$$Vd(\alpha) := Vd1(\alpha)+Vd2(\alpha)-Vd3(\alpha)$$

$$\alpha := 0\cdot deg, 1\cdot deg .. 165\cdot deg$$

$xxx := READPRN(ccc)$ We may read EMTDC generated file ccc.prn for comparison

$alfa := xxx^{\langle 2\rangle}$

$Vdc := xxx^{\langle 1\rangle}\cdot(-.5)$ $\quad j := 0, 1 .. last(alfa)$

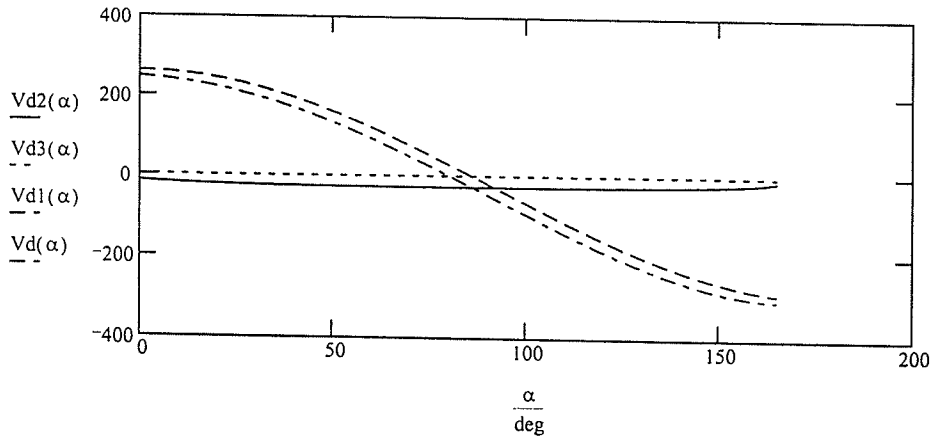

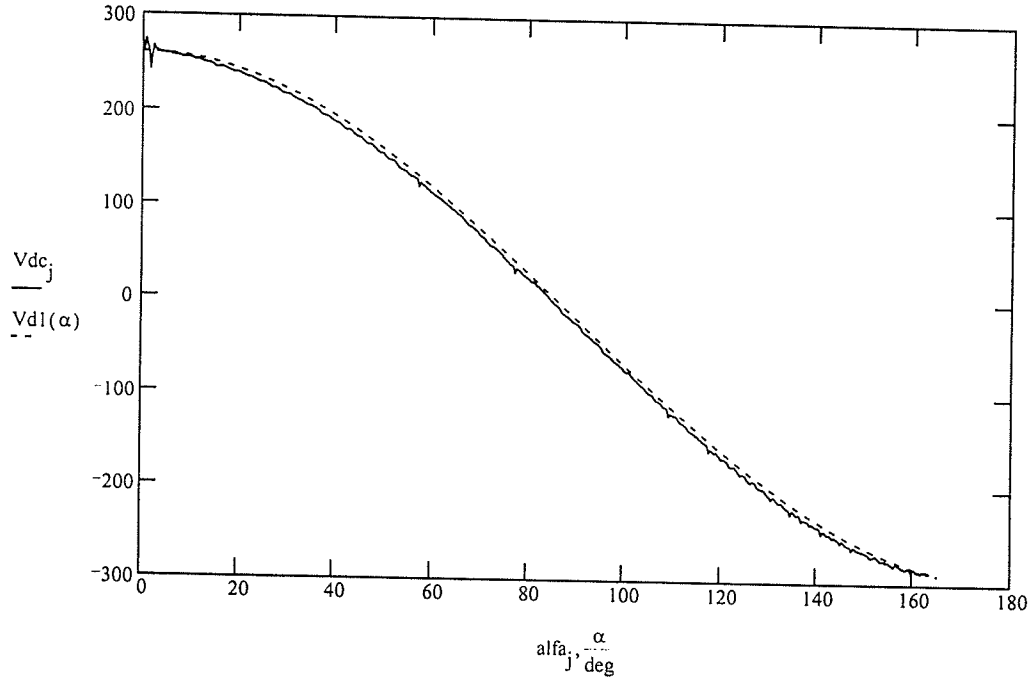
300
200
100
0
-100
-200
-300
0
20
40
60
80
100
120
140
160
180
Vdc_j
Vdl(α)
alfa_j, α deg

Appendix C

Gamma Measurement Component

The definition and subroutine of the gamma measurement block is shown below.

1(a) Definition for 1 Input Block

```
PARAMETERS:
    Fre     "Frequency"  "Hz "  10 REALVAR   60.0 0.0 100.0
GRAPHICS:
    BOX (-40,-40,40,40)
    LINE ( 40,  0, 64,  0)  FTEXT( 25,  0,"GMES")   ARROW_R( 64,  0)
    LINE (-64,-32,-40,-32)  FTEXT(-24,-32,"VALVE")  ARROW_R(-40,-32)
    LINE (-64, 32,-40, 32)  FTEXT(-25, 32,"LINE")   ARROW_R(-40, 32)
    LINE (-64,  0,-40,  0)  FTEXT(-24,  0,"t1")     ARROW_R(-40,  0)
NODES:
    valve   -2 -1 INPUT  INTEGER
    linex   -2  1 INPUT  INTEGER
    t1      -2  0 INPUT  INTEGER
    gmes     2  0 OUTPUT REAL
FORTRAN: DSD
    C Generate measured gamma from valve and line voltage zero X
        CALL gammes($valve,$linex,$gmes,$t1,$Fre,ifl_g)
```

FILES:

gammes.f

1(b) Definition for 6 Input Block

PARAMETERS:

Fre "Frequency" "Hz " 10 REALVAR 60.0 0.0 100.0

GRAPHICS:

BOX (-40,-40,40,40)

LINE (40, 0, 64, 0) FTEXT(25, 0,"Gmin") ARROW_R(64, 0)

LINE (40, 32, 64, 32) FTEXT(25, 32,"Gmes") ARROW_R(64, 32)

LINE (-64,-32,-40,-32) FTEXT(-24,-32,"VALVE") ARROW_R(-40,-32)

LINE (-64, 32,-40, 32) FTEXT(-25, 32,"LINE") ARROW_R(-40, 32)

LINE (-64, 0,-40, 0) FTEXT(-24, 0,"t1") ARROW_R(-40, 0)

NODES:

valve -2 -1 INPUT INTEGER 6

linex -2 1 INPUT INTEGER 6

t1 -2 0 INPUT INTEGER 6

gmin 2 0 OUTPUT REAL

gmes 2 1 OUTPUT REAL

FORTRAN: DSD

```
#DEFINE REAL g_m(6)
#DEFINE INTEGER ifl_g
C Generate measured gamma from valve and line voltage zero X
    nxgms=nexc+1
    nexc = nexc+1
   DO J = 1,6
   CALL gammes($valve(J),$linex(J),g_m(J),$t1(J),$Fre,ifl_g)
    IF(ifl_g.EQ.1) THEN
     $gmes = g_m(J)
     stor(nxgms)=g_m(J)
    ELSE
     $gmes = STOR(nxgms)
   END IF
```

```
        END DO
        $gmin=amin1(g_m(1),g_m(2),g_m(3),g_m(4),g_m(5),g_m(6))
FILES:
    gammes.f
```

2 Subroutine

```
      SUBROUTINE gammes(valve,linex,gmes,t1,fre,ifl_g)
C23456789 C23456789 C23456789 C23456789 C23456789 C23456789 C23456789
C     To measure gamma from pulse width of SR Bistable
C     Date 16 April 1996
C     By Amir Hashim
C     Include & common block declarations
      INCLUDE 'emt.d'
      INCLUDE 'emt.e'
      COMMON/S1/TIME,DELT,ICH,PRINT,FINTIM
      COMMON/S2/STOR(ND10),NEXC

C     Variable Declarations
      REAL delt,fre
      REAL spulse,epulse,fintim
      REAL gtime,gmes
      INTEGER init,selecta,selectb,valve,linex,t1,trig
      INTEGER ICH,NEXC
C     Variable Definitions
C     init = flag showing that pulse has started
C     spulse = Start of Pulse
C     epulse = End of Pulse
C     t1     = thyristor 1 firing
C     trig   = flag showing t1 has fired
C-------------------------------------------------------------------------
C Initialising flag for determining pulse start/detecting pulse phase
      ifl_g = 0
      IF (time.LE.delt) then
            selecta = 0
            selectb = 0
            init = 0
            spulse = 0
            gmes = 0
            trig = 0
      ELSE
            spulse=stor(NEXC+1)
            init=stor(NEXC+2)
            selecta=stor(NEXC+3)
```

```
            selectb=stor(NEXC+4)
            gmes = stor(NEXC+5)
            trig = stor(NEXC+6)
        ENDIF
C_____________________________________________________________________
C       Zero crossing of valvol and linvol
C
C       valve = -IZCD1(valvol,DT)
C       linex = IZCD1(linvol,DT)
C_____________________________________________________________________
C       To detect firing of thyristor 1 to make counter wait for zero
C       crossing

        IF (t1.GE.0.95) THEN
            trig = 1
        ENDIF
C_____________________________________________________________________
C       To detect start time of gamma depending on whether
C       valve voltage or line voltage crosses zero first with respect
C       to firing of valve 1

        IF (trig.GE.0.95) THEN
            IF (valve.GE.0.95.AND.init.LE.0.AND.linex.LE.0) THEN
                selecta = 1
                init = 1
                spulse = time
            ELSEIF (valve.LE.0.AND.init.LE.0.AND.linex.GE.0.95)
     .THEN
                selectb = 1
                init = 1
                spulse = time
            ENDIF
C_____________________________________________________________________
C       To detect end time of gamma
            IF (selecta.GE.1.AND.init.GE.1.AND.linex.GE.0.95) THEN
                epulse = time
                gtime = epulse - spulse

            ELSEIF (valve.LE.0.AND.init.LE.0.AND.linex.GE.0.95)
     .THEN
                selectb = 1
                init = 1
                spulse = time
            ENDIF
C_____________________________________________________________________
C       To detect end time of gamma
            IF (selecta.GE.1.AND.init.GE.1.AND.linex.GE.0.95) THEN
                epulse = time
```

```
            gtime = epulse - spulse
            gmes = gtime*(360*fre)
            init = 0
            selecta = 0
            trig = 0
            ifl_g = 1
        ELSEIF  (selectb.GE.1.AND.init.GE.1.AND.valve.GE.0.95)
.THEN
            epulse = time
            gtime = epulse - spulse
            gmes = gtime*(-360*fre)
            init = 0
            selectb = 0
            trig = 0
            ifl_g = 1
        ENDIF
 ENDIF

        stor(NEXC+1)=spulse
        stor(NEXC+2)=init
        stor(NEXC+3)=selecta
        stor(NEXC+4)=selectb
        stor(NEXC+5)=gmes
        stor(NEXC+6)=trig

        NEXC = NEXC + 6

 RETURN
 END
```

Appendix D

PSCAD Draft Files

a) Gamma Measurement

b) Modulation Circuit

c) Active Filter Controls

d) Inverter Controls

e) Rectifier Controls

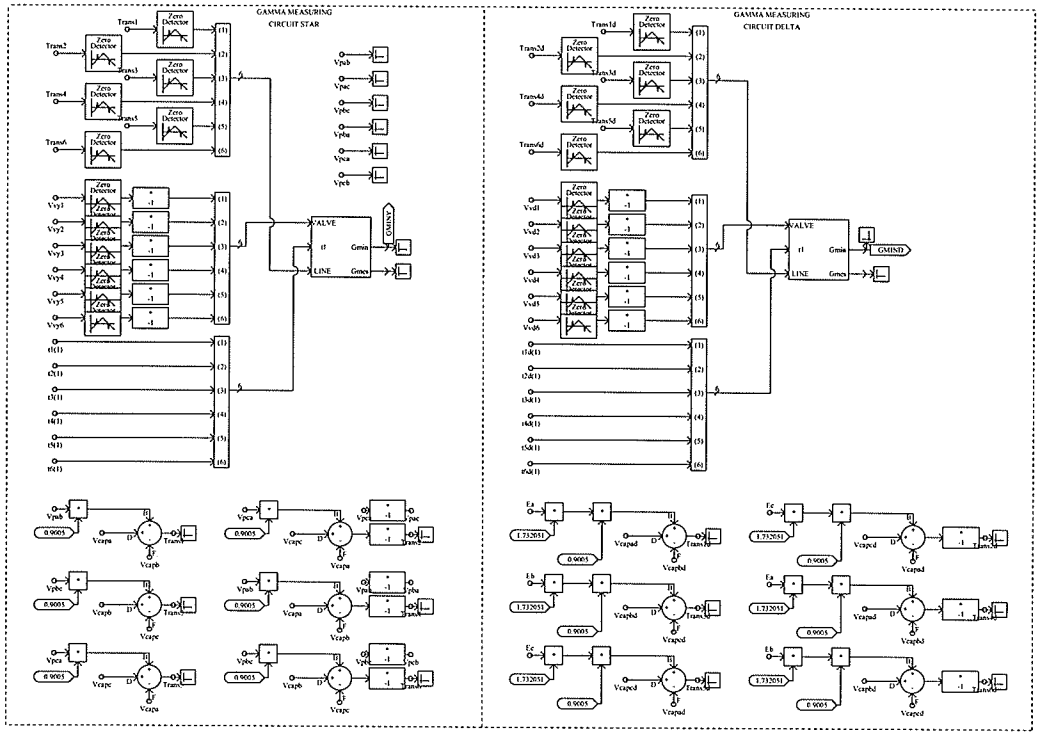

University of Manitoba, EE Dept. *Gamma Measurement Circuit*	Created: September 11, 1996 (hashim) Last Modified: September 11, 1996 (hashim) Printed On: October 08, 1996 (hashim)	*SS 1*

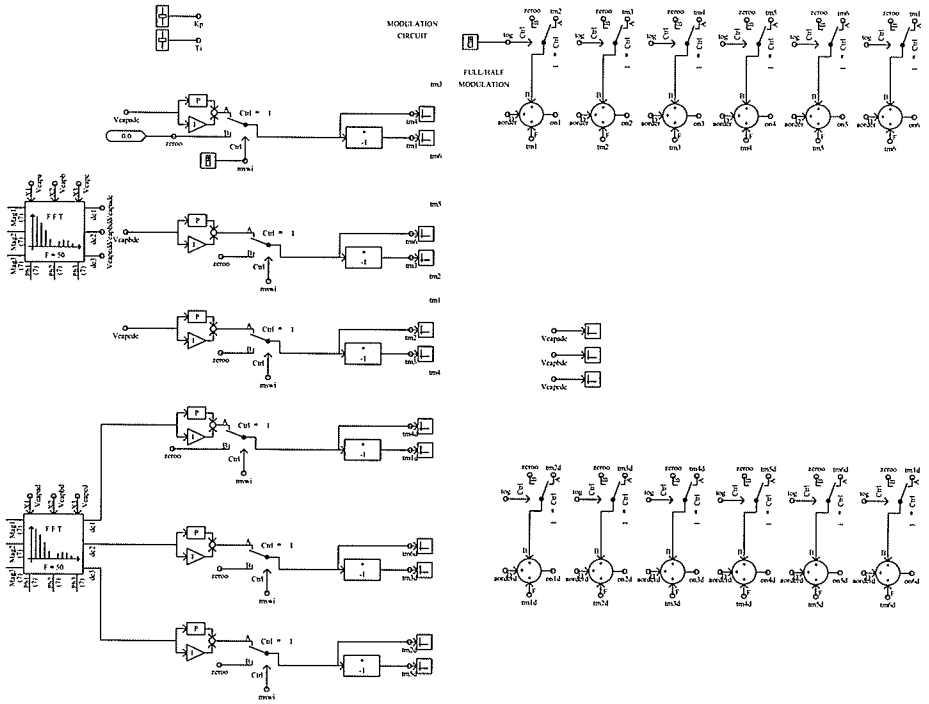

University of Manitoba, EE Dept. *Modulation Circuit*	Created: September 11, 1996 (hashim) Last Modified: September 11, 1996 (hashim) Printed On: October 08, 1996 (hashim)	*SS 1*

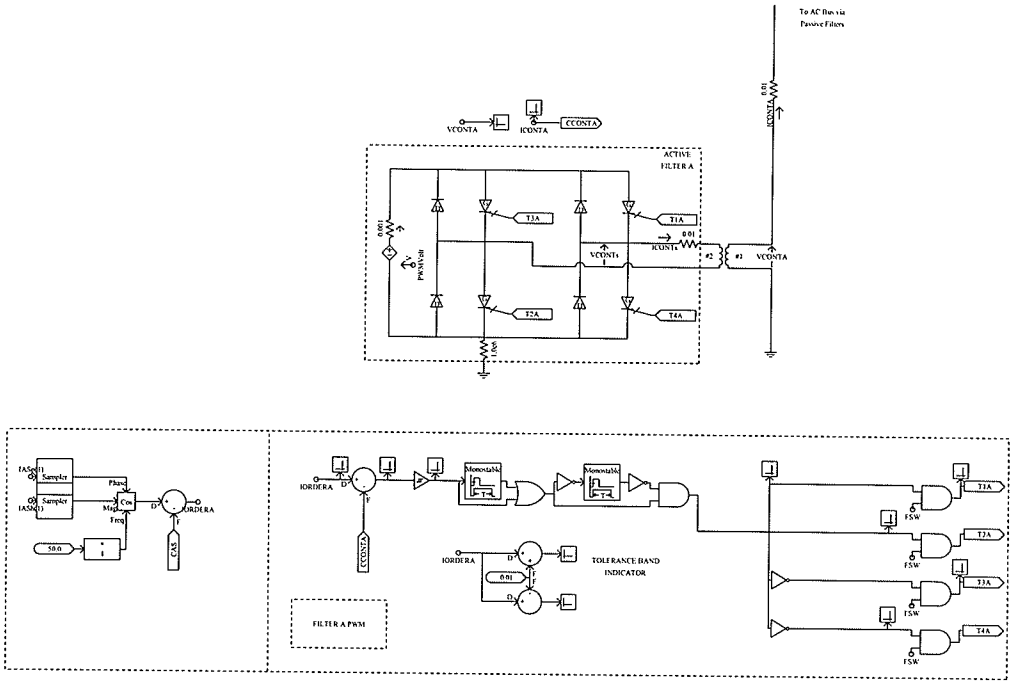

University of Manitoba, EE Dept. *Active Filter Injection and Controls*	Created: September 11, 1996 (hashim) Last Modified: September 11, 1996 (hashim) Printed On: October 08, 1996 (hashim)	*SS 1*

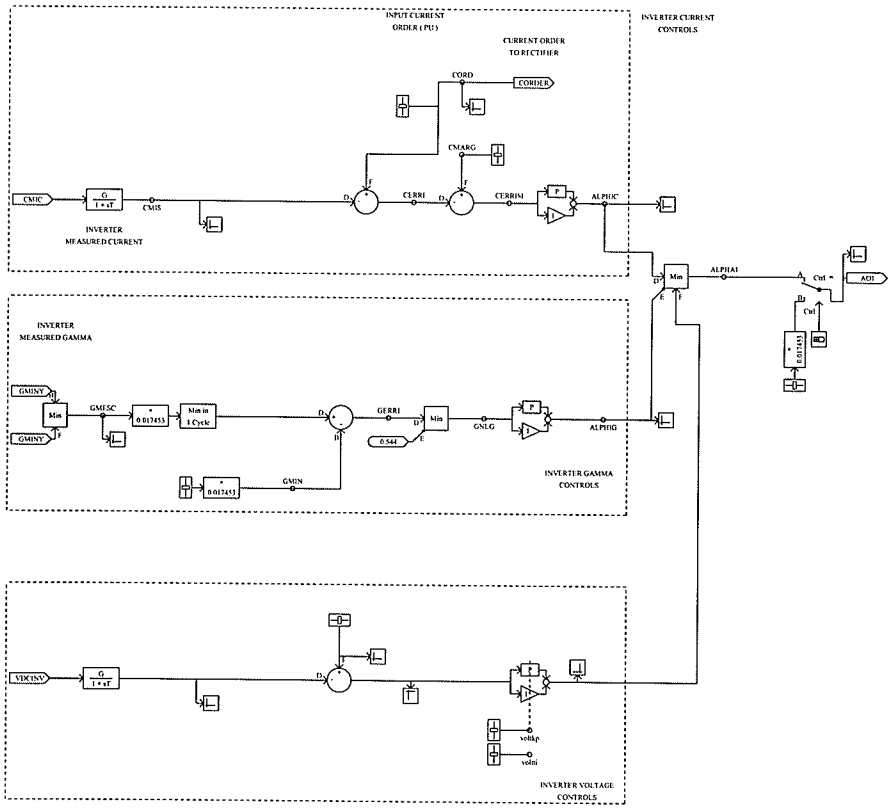

University of Manitoba, EE Dept. *Inverter Controls*	Created: September 11, 1996 (hashim) Last Modified: September 11, 1996 (hashim) Printed On: October 08, 1996 (hashim)	*SS 1*

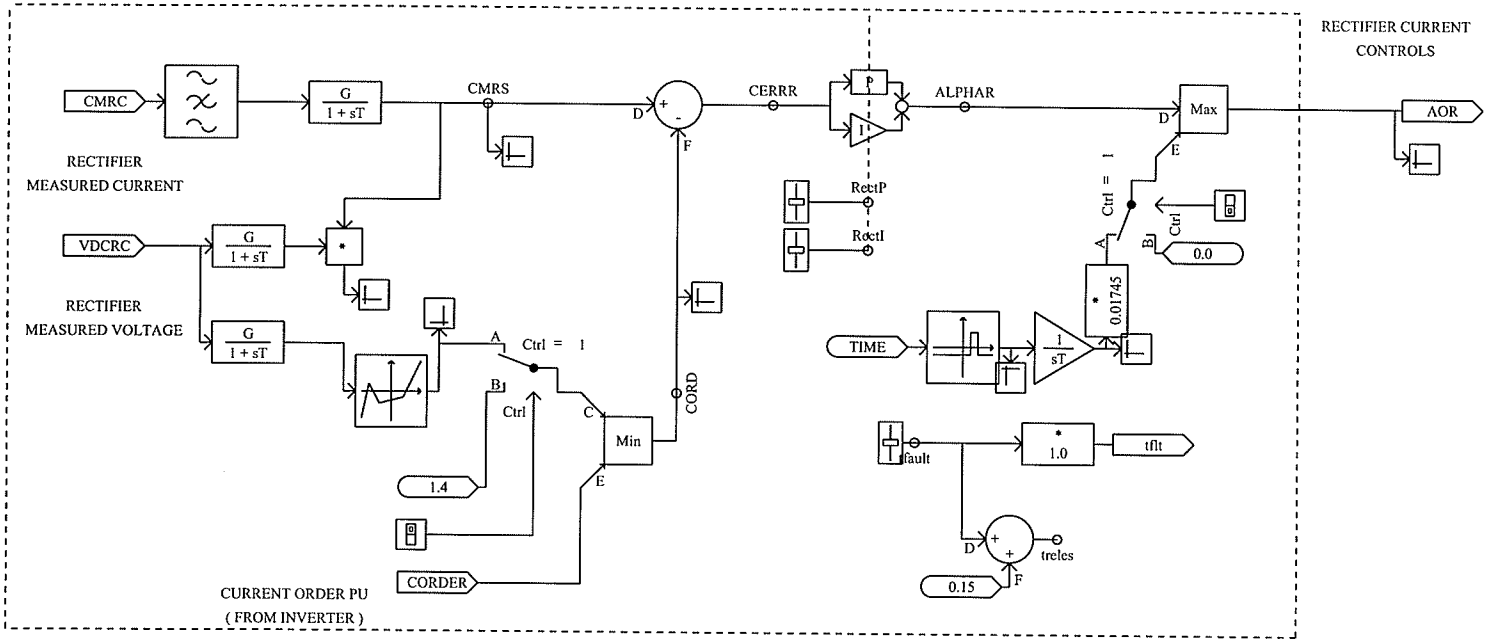

University of Manitoba, EE Dept. *Rectifier Controls*	Created: September 11, 1996 (hashim) Last Modified: September 11, 1996 (hashim) Printed On: October 08, 1996 (hashim)	*SS 1*